SUPPORTING INFORMATION

Supporting Information

69451 Weinheim, Germany

Sterically Shielded Heptamethine Cyanine Dyes for Bioconjugation and High Performance Near-Infrared Fluorescence Imaging

Dong-Hao Li, Cynthia L. Schreiber, Bradley D. Smith*

Abstract: The near-infrared window of fluorescent heptamethine cyanine dyes greatly facilitates biological imaging because there is deep penetration of the light and negligible background fluorescence. But dye instability, aggregation, and poor pharmacokinetics are current drawbacks that limit performance and the scope of possible applications. All these limitations are simultaneously overcome with a new molecular design strategy that produces a charge balanced and sterically shielded fluorochrome. The key design feature is a meso-Aryl group that simultaneously projects two shielding arms directly over each face of a linear heptamethine polyene. Cell and mouse imaging experiments compared a shielded heptamethine cyanine dye (and several peptide and antibody bioconjugates) to benchmark heptamethine dyes and found that the shielded systems possess an unsurpassed combination of photophysical, physiochemical and biodistribution properties that greatly enhance bioimaging performance.

DOI: 10.1002/anie.2016XXXXX

SUPPORTING INFORMATION

Table of Contents

1. General……3

2. Synthesis……4-15

3. Solubility Differences……16

4. NMR Spectra of s775z and Related Dyes……17-18

5. Bioconjugation……19-21

6. Photophysical Properties……22

7. Absorption, Excitation and Emission Spectra of s775z and 755z……23-25

8. Chemical Stability, pH Independence, and Albumin Binding ……26-27

9. Photostability Measurements……28-30

10. Synthesis and Characterization of s775z-IgG and 756z-IgG……31-34

11. Cell Experiments……35-36

12. Mouse Biodistribution……37

13. Mouse Tumor Imaging……38-39

14. Molecular Modeling……40-43

References……44

Author Contributions……44

SUPPORTING INFORMATION

1. General

Reagents and solvents were purchased from Sigma-Aldrich, VWR, Oakwood, Thermo Fisher and TCI and used without further purification unless stated otherwise. Anhydrous tetrahydrofuran was distilled with metal sodium and benzophenone. Column chromatography was performed using Biotage SNAP Ultra columns. ^{1}H, ^{13}C and ROESY NMR spectra were recorded on a Bruker 500 NMR spectrometer. Chemical shifts are presented in ppm and referenced by residual solvent peak. High-resolution mass spectrometry (HRMS) was performed using a time-of-flight (TOF) analyzer with electrospray ionization (ESI). Absorption spectra were recorded on an Evolution 201 UV/vis spectrometer with Thermo Insight software. Fluorescence spectra were collected on a Horiba Fluoromax-4 fluorometer with FluoroEssence software. Analyte solutions were prepared in HPLC grade water (Sigma-Aldrich), phosphate buffered saline (Thermo Fisher), fetal bovine serum (Sigma-Aldrich) or buffer B (575 mM NaCl, 37.5 mM NaH_2PO_4 and 0.75 mM EDTA in water, pH 7.5). All absorption and fluorescence spectra were collected using quartz cuvettes (1 mL, 1 cm path length; for emission and excitation spectra, slit width = 3 nm).

2. Synthesis

Synthetic Scheme to Make **s775z**

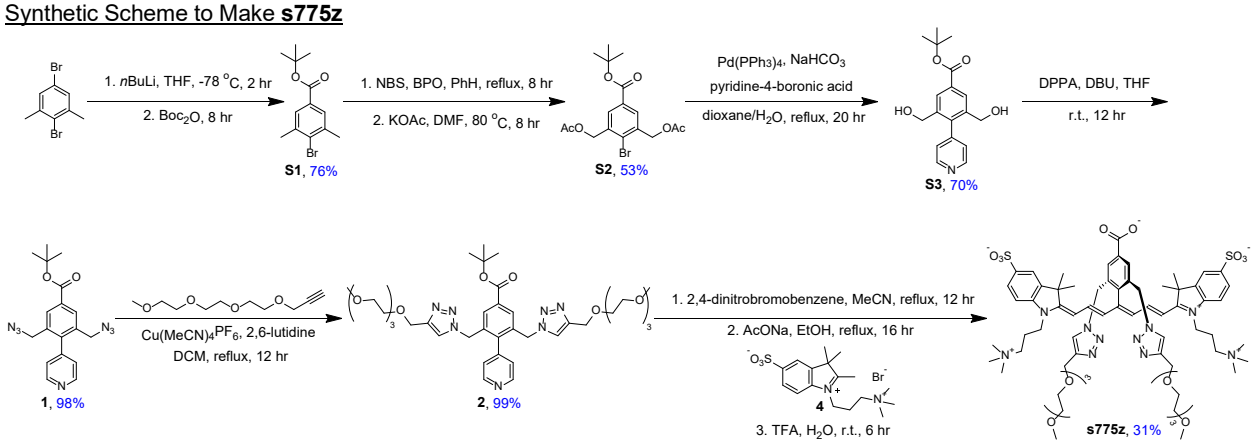

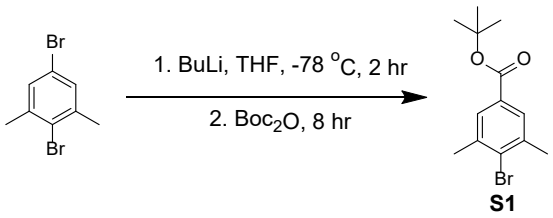

Compound **S1**.[1] Compound 2,5-dibromo-m-xylene (5.00 g, 18.9 mmol, 1 eq) was dissolved in fresh distilled THF (50 mL). The clear yellow solution was chilled to -78 °C in a dry ice-acetone bath. Air was expelled and refilled with argon using vacuum line. *n*-Butyl lithium (1.6 M in hexane, 13.0 mL, 20.8 mmol, 1.1 eq) was added dropwise into the solution and gave a cloudy brown mixture. The mixture was stirred at the same temperature for 2 hr. Di-*tert*-butyl dicarbonate (4.96 g, 22.7 mmol, 1.2 eq) in dry THF (10 mL) was added dropwise. The mixture was allowed to warm to r.t. and at this time it turned clear again. The mixture was stirred for 4 hr at r.t. then quenched with 5 % aq. HCl (50 mL). The mixture was extracted with DCM (3 x 50 mL). The organic extracts were dried over anhydrous sodium sulfate, filtered. Solvent was removed under reduced pressure and the residue was purified by column chromatography (SiO_2, 0-5% EtOAc in hexane) to afford **S1** as a white solid (4.1 g, 76 %, R_f = 0.6 in hexane/EtOAc = 10/1). ^{1}H NMR (500 MHz, $CDCl_3$, 25 °C) δ (ppm): 7.67 (s, 2H), 2.45 (s, 6H), 1.59 (s, 9H).

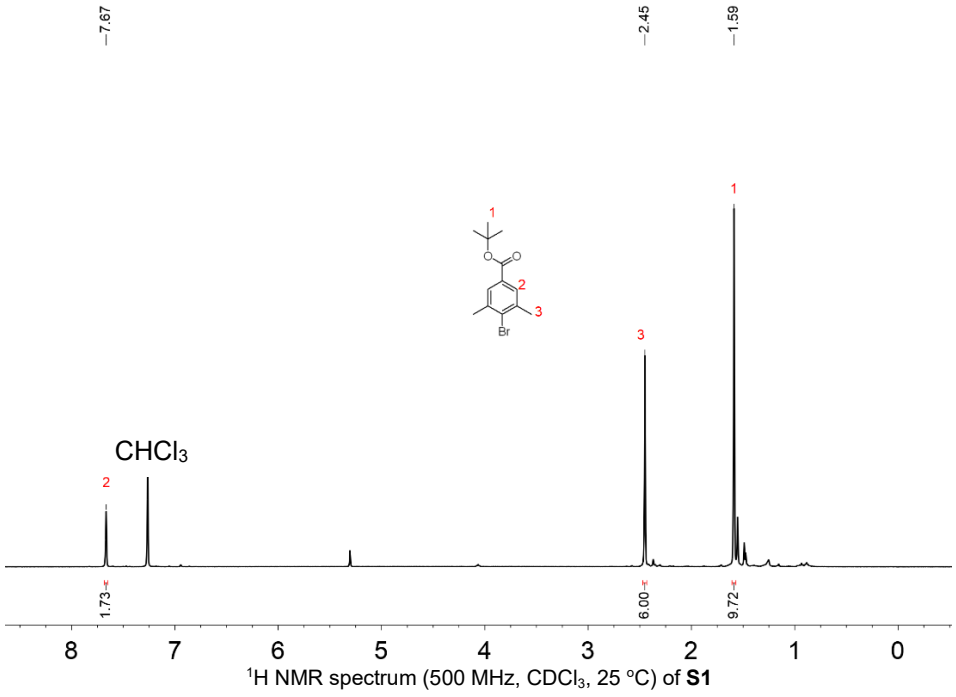

^{1}H NMR spectrum (500 MHz, $CDCl_3$, 25 °C) of **S1**

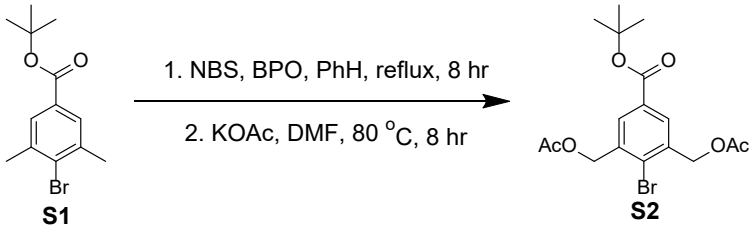

S1 **S2**

Compound **S2**. A mixture of **S1** (1.00 g, 3.51 mmol, 1 eq), *N*-bromosuccinimide (1.37 g, 7.71 mmol, 2.2 eq) and benzoyl peroxide (42.5 mg, 175 µmol, 0.05 eq) in benzene (50 mL) was refluxed for 8 hr under argon atmosphere. Solvent was removed under reduced pressure. Hexane (100 mL) was added to the residue then the brown solid was removed by filtration. The filtrated was evaporated under reduced pressure to give the crude diBr intermediate as a brown oil. A mixture of the crude diBr intermediate and potassium acetate (2.06 g, 21.0 mmol, 6 eq) in anhydrous DMF (20 mL) was stirred at 80 °C for 8 hr. The mixture was diluted with water (100 mL) and extracted with DCM (3 x 100 mL). The organic extracts were dried over anhydrous sodium sulfate, then filtered. Solvent was removed under reduced pressure and the residue was purified by column chromatography (SiO_2, 0-15% EtOAc in hexane) to afford **S2** as a white solid (740 mg, 53 %, R_f = 0.4 in hexane/EtOAc = 4/1). ^{1}H NMR (500 MHz, $CDCl_3$, 25 °C) δ (ppm): 7.96 (s, 2H), 5.24 (s, 4H), 2.18 (s, 6H), 1.60 (s, 9H). ^{13}C NMR (126 MHz, $CDCl_3$, 25 °C) δ (ppm): 170.7, 164.7, 136.6, 131.5, 129.9, 128.7, 82.1, 65.9, 28.3, 21.1. HRMS (ESI-TOF) m/z: $[M + Na]^+$ calcd for $C_{17}H_{21}BrNaO_6^+$ 423.0414, found 423.0414. This reaction gave ~30% monoacetate byproduct.

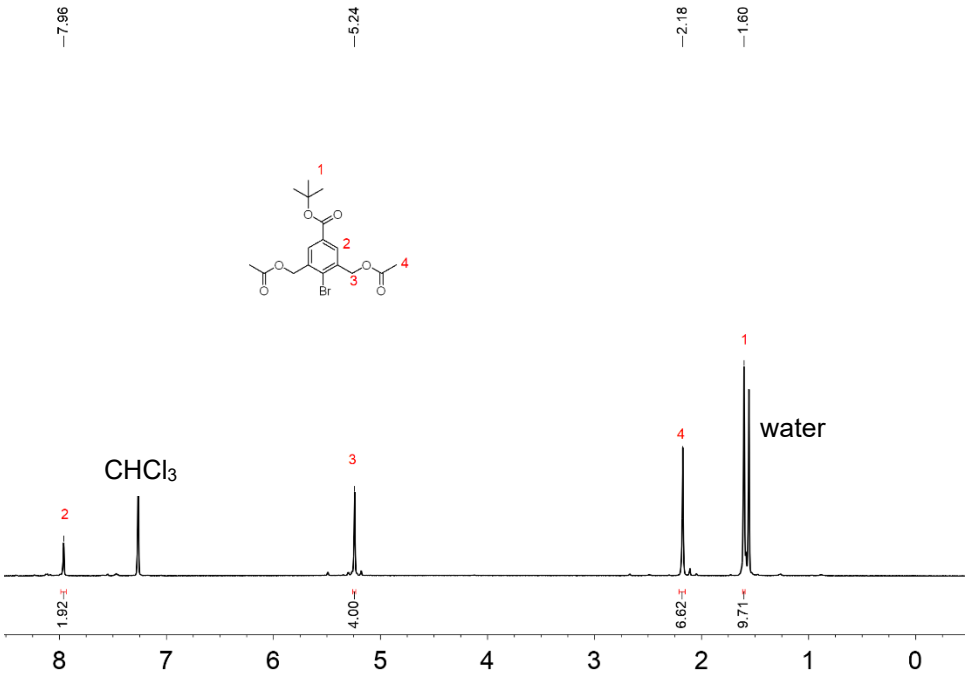

^{1}H NMR spectrum (500 MHz, $CDCl_3$, 25 °C) of **S2**

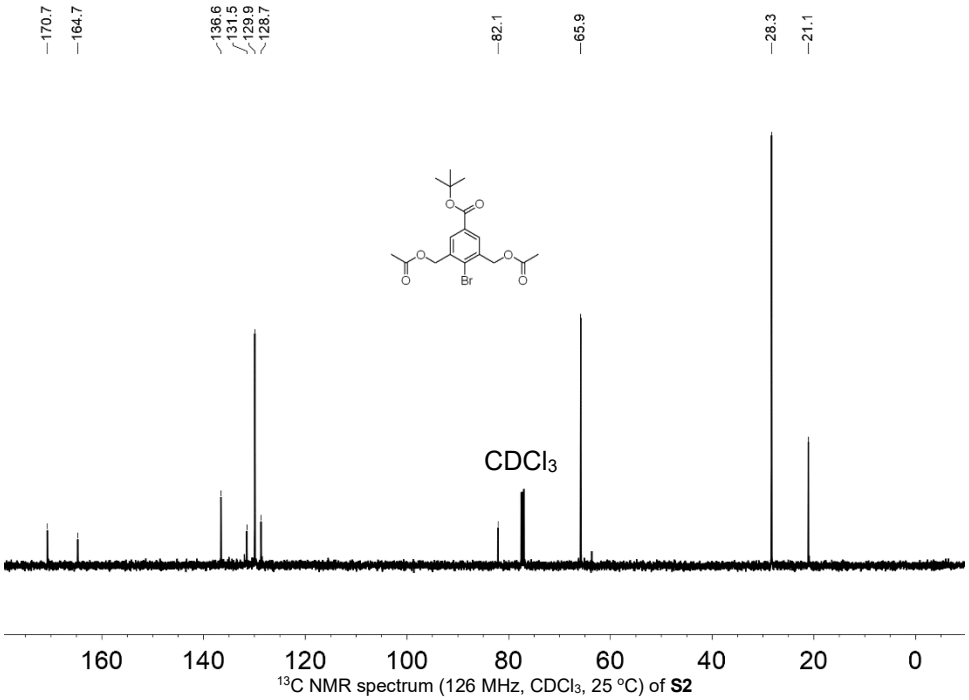

^{13}C NMR spectrum (126 MHz, $CDCl_3$, 25 °C) of **S2**

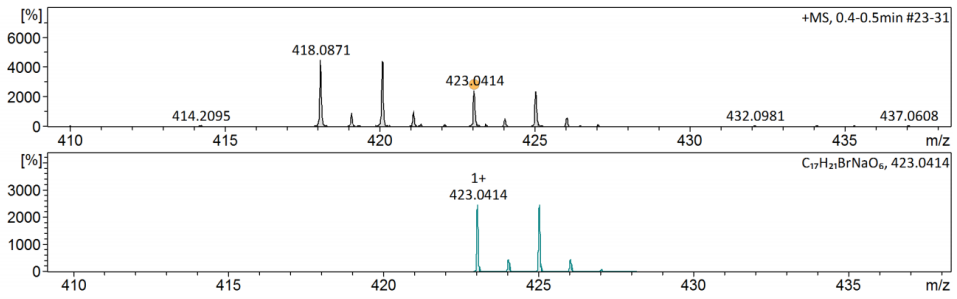

Meas. m/z	#	Ion Formula	m/z	err [ppm]	Mean err [ppm]	rdb	N-Rule	e⁻ Conf
423.041355	1	C17H21BrNaO6	423.041371	0.0	-0.1	6.5	ok	even

HRMS (ESI-TOF) spectrum of **S2**

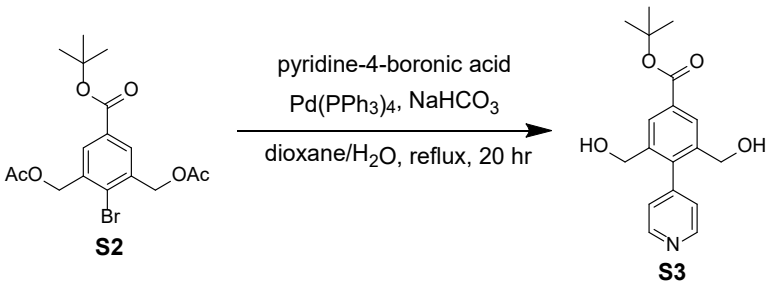

S2 **S3**

Compound **S3**. A mixture of **S2** (200 mg, 498 µmol, 1 eq), pyridine-4-boronic acid (184 mg, 1.50 mmol, 3 eq) and $Pd(PPh_3)_4$ (28.8 mg, 24.9 µmol, 5 mol%) in 1,4-dioxane (6 mL) and sat. $NaHCO_3$ (3 mL) was refluxed for 20 hr. The mixture was diluted with sat. aq. NaCl (30 mL) and extracted with EtOAc (3 x 30 mL). The organic extracts were dried over anhydrous sodium sulfate, filtered. Solvent was removed under reduced pressure and the residue was purified by column chromatography (SiO_2, 0-8% MeOH in DCM) to afford **S3** as a brown solid (100 mg, 70 %, R_f = 0.5 in DCM / MeOH = 10/1). ^{1}H NMR (500 MHz, DMSO-d_6, 25 °C) δ (ppm): 8.64 (d, J = 3.5 Hz, 2H), 8.01 (s, 2H), 7.22 (d, J = 3.5 Hz, 2H), 5.23 (t, J = 4.9 Hz, 2H), 4.11 (d, J = 4.9 Hz, 4H), 1.56 (s, 9H). ^{13}C NMR (126 MHz, DMSO-d_6, 25 °C) δ (ppm): 165.8, 150.4, 145.9, 140.4, 140.0, 131.5, 126.7, 124.6, 81.4, 61.1, 28.5. HRMS (ESI-TOF) m/z: $[M + H]^+$ calcd for $C_{18}H_{22}NO_4^+$ 316.1543, found 316.1541.

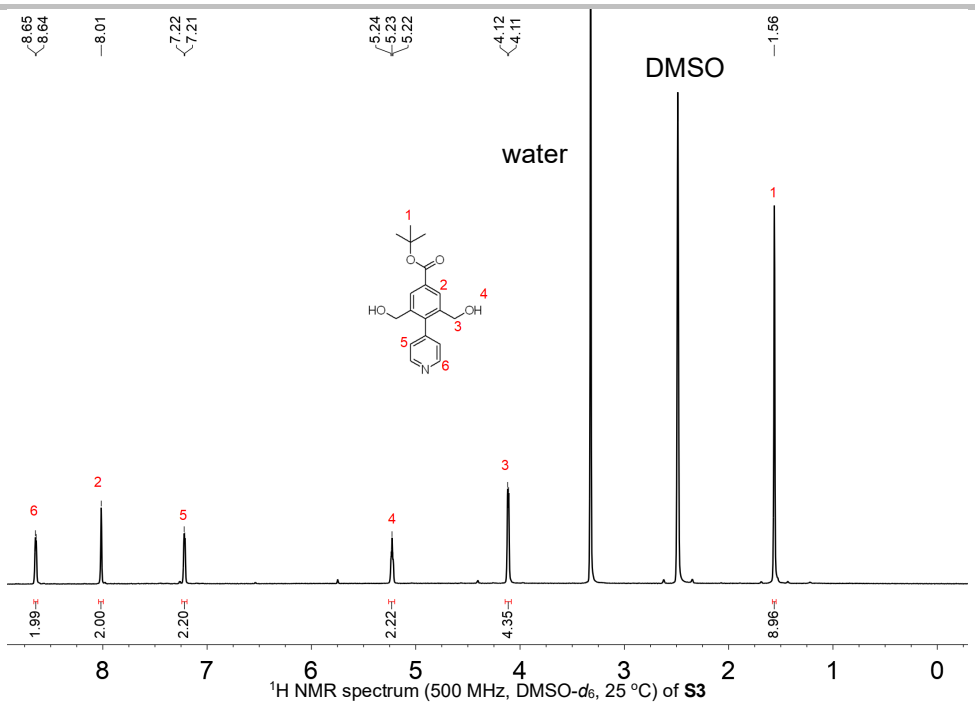

^{1}H NMR spectrum (500 MHz, DMSO-d_6, 25 °C) of **S3**

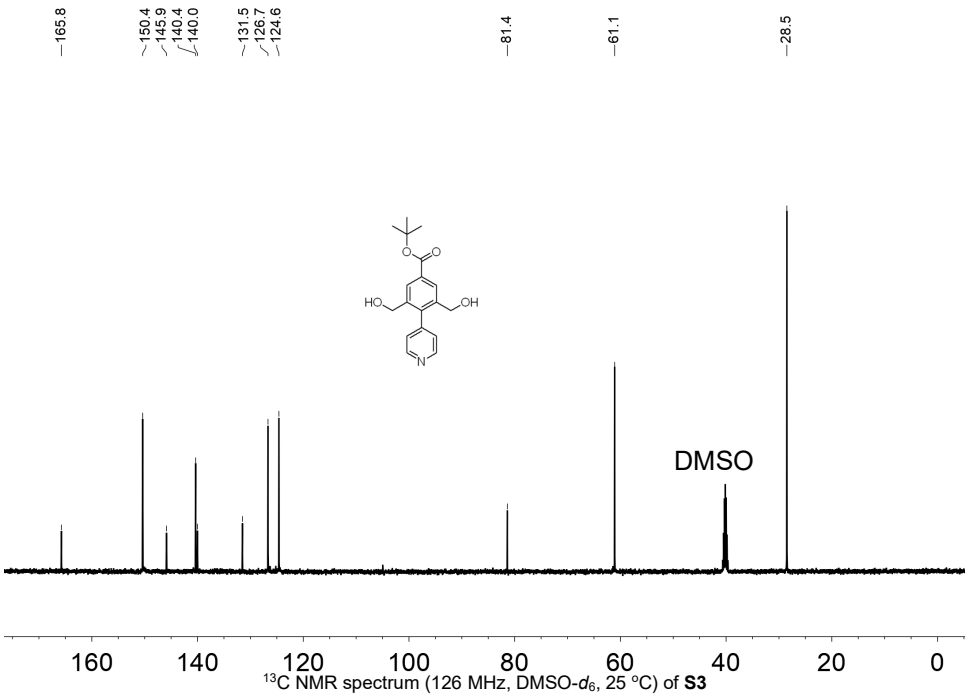

^{13}C NMR spectrum (126 MHz, DMSO-d_6, 25 °C) of **S3**

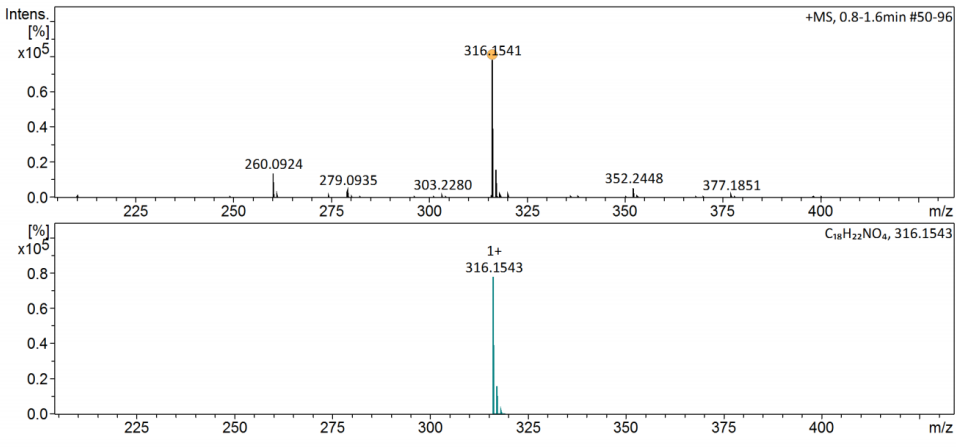

Meas. m/z	#	Ion Formula	m/z	err [ppm]	Mean err [ppm]	rdb	N-Rule	e⁻ Conf
316.154130	1	C18H22NO4	316.154335	0.6	1.0	8.5	ok	even

HRMS (ESI-TOF) spectrum of **S3**

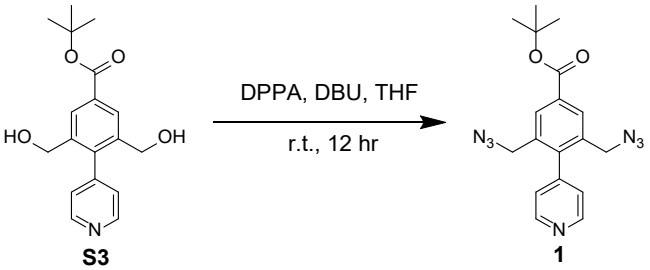

S3 **1**

Compound **1**. To a solution of **S3** (300 mg, 951 µmol, 1 eq) in THF (10 mL) was added diphenylphosphoryl azide (0.614 mL, 2.85 mmol, 3 eq) and 1,8-diazabicyclo[5.4.0]undec-7-ene (0.426 mL, 2.85 mmol, 3 eq). The mixture was stirred at room temperature for 12 hr. Solvent was removed and the residue was purified by flash column chromatography (SiO_2, 10-40% EtOAc in hexane) to afford **1** as a yellow solid (340 mg, 98 %, R_f = 0.4 in hexane/EtOAc = 1/1). ^{1}H NMR (500 MHz, $CDCl_3$, 25 °C) δ (ppm): 8.82 (d, *J* = 5.5 Hz, 2H), 8.08 (s, 2H), 7.44 (d, *J* = 5.5 Hz, 2H), 4.11 (s, 4H), 1.64 (s, 9H). ^{13}C NMR (126 MHz, $CDCl_3$, 25 °C) δ (ppm): 164.6, 150.5, 145.1, 142.8, 134.4, 133.1, 130.5, 124.2, 82.3, 52.5, 28.4. HRMS (ESI-TOF) m/z: $[M + H]^+$ calcd for $C_{18}H_{20}N_7O_2^+$ 366.1673, found 366.1667.

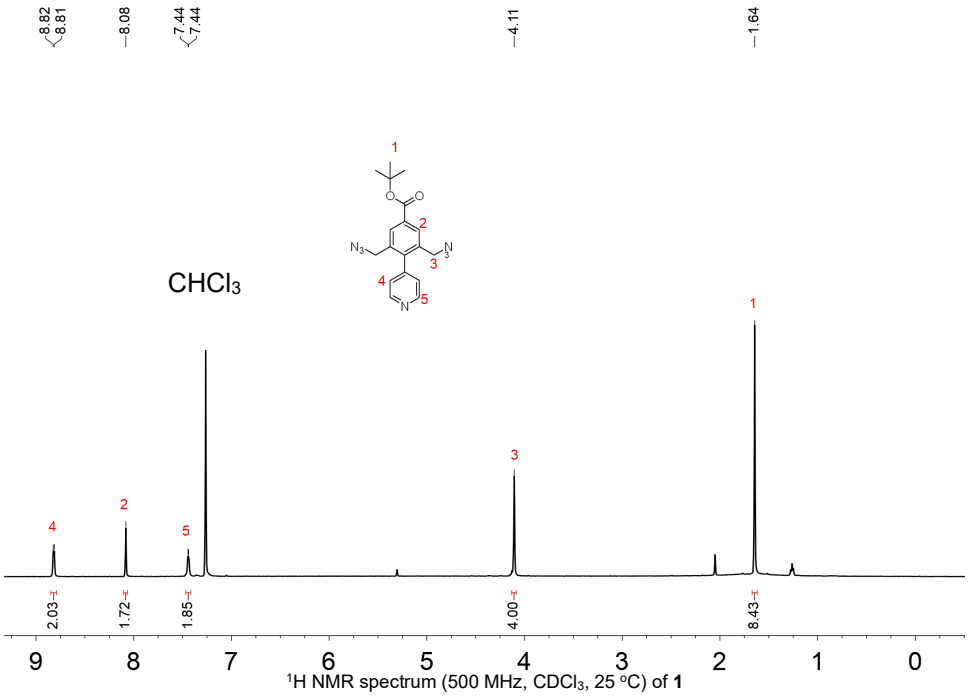

^{1}H NMR spectrum (500 MHz, $CDCl_3$, 25 °C) of **1**

SUPPORTING INFORMATION

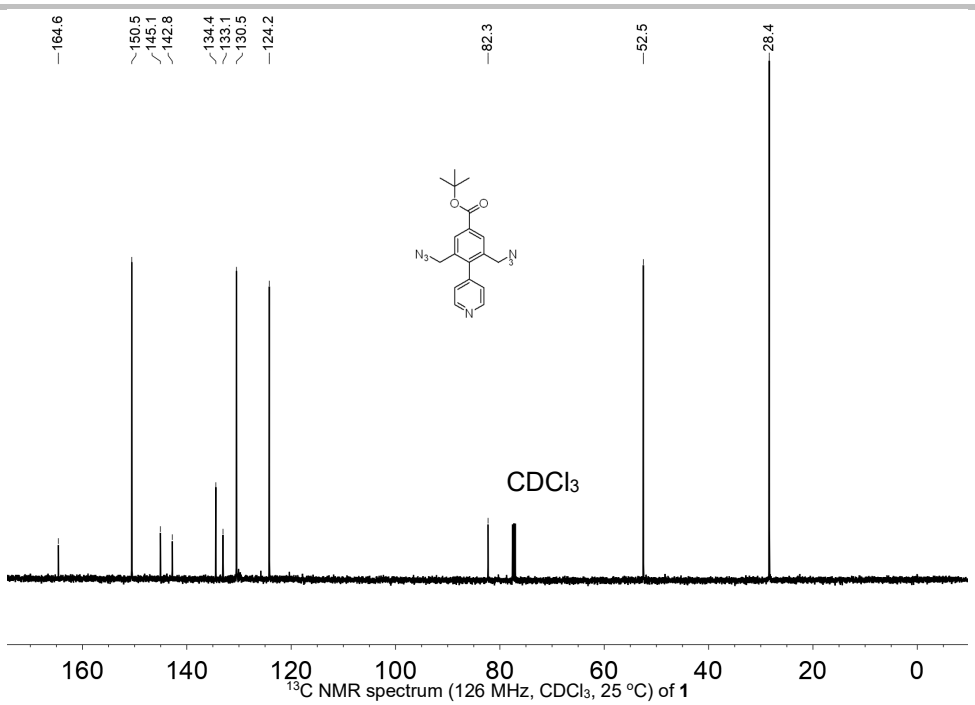

^{13}C NMR spectrum (126 MHz, $CDCl_3$, 25 °C) of **1**

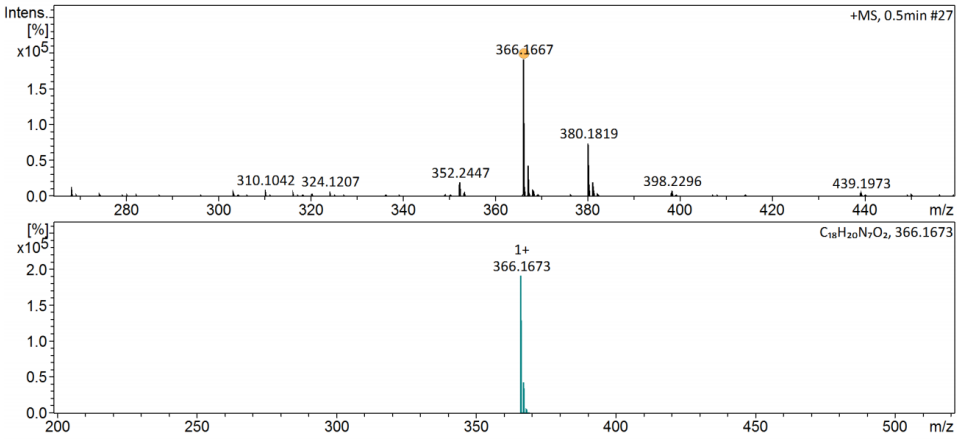

Meas. m/z	#	Ion Formula	m/z	err [ppm]	Mean err [ppm]	rdb	N-Rule	e⁻ Conf
366.166681	1	C18H20N7O2	366.167299	1.7	1125.4	12.5	ok	even

HRMS (ESI-TOF) spectrum of **1**

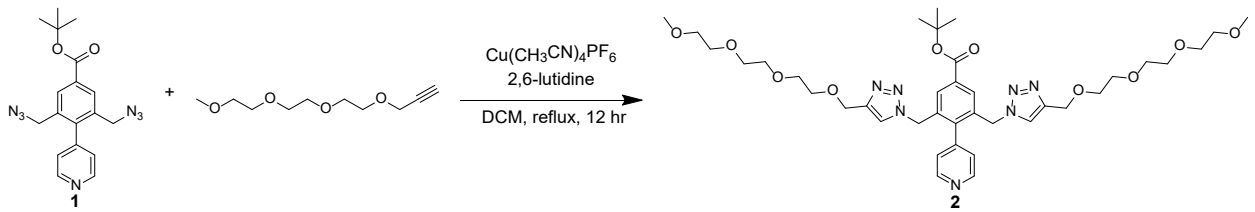

Compound **2**. A mixture of **1** (150 mg, 411 µmol, 1 eq), triethylene glycol methyl propargyl ether (249 mg, 1.23 mmol, 3 eq), $Cu(MeCN)_4PF_6$ (7.65 mg, 20.5 µmol, 0.05 eq) and one drop of 2,6-lutidine in DCM (10 mL) was refluxed under argon atmosphere overnight. Solvent was removed and the residue was purified by flash column chromatography (SiO_2, 0-8% MeOH in DCM) to afford **2** as a brown oil (316 mg, 99%, Rf = 0.4 in DCM/MeOH = 10/1). ^{1}H NMR (500 MHz, DMSO-d_6, 25 °C) δ (ppm): 8.60 (s, 2H), 7.79 (d, J = 1.9 Hz, 2H), 7.72 (d, J = 1.9 Hz, 2H), 7.08 (s, 2H), 5.33 (s, 4H), 4.45 (s, 4H), 3.50 - 3.39 (m, 24H), 3.20 (s, 6H), 1.50 (s, 9H).^{13}C NMR (126 MHz, DMSO-d_6, 25 °C) δ (ppm): 164.5, 150.5, 150.4, 144.7, 143.0, 135.2, 132.4, 130.9, 129.9, 125.1, 82.1, 71.9, 70.5, 70.4, 70.3, 70.2, 69.5, 64.0, 58.7, 51.3, 28.3. HRMS (ESI-TOF) m/z: $[M + H]^+$ calcd for $C_{38}H_{56}N_7O_{10}^+$ 770.4083, found 770.4086.

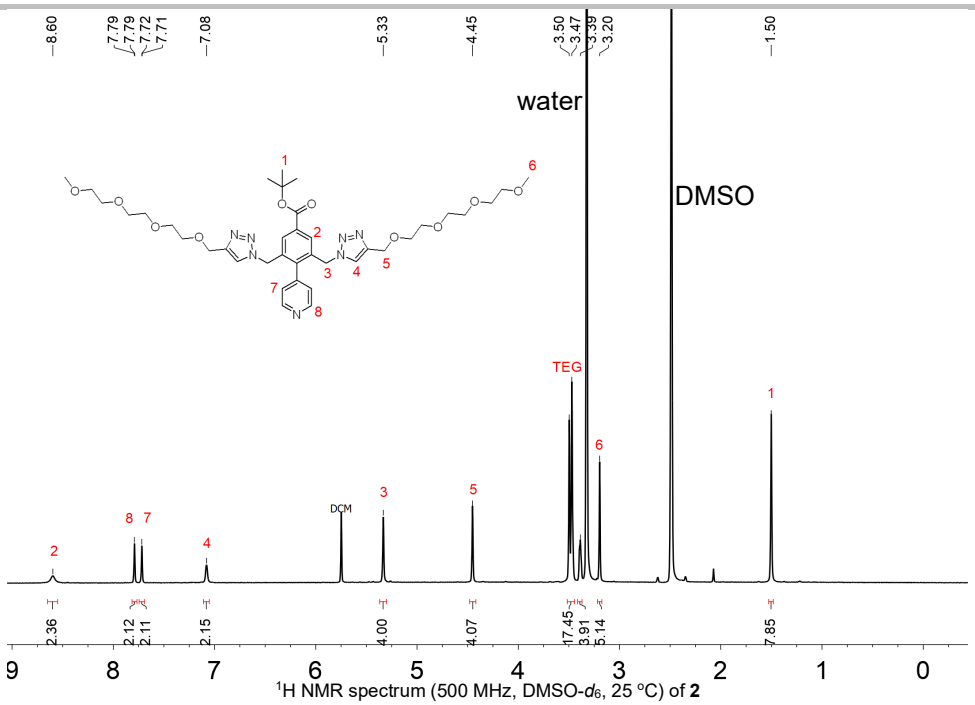

^{1}H NMR spectrum (500 MHz, DMSO-d_6, 25 °C) of **2**

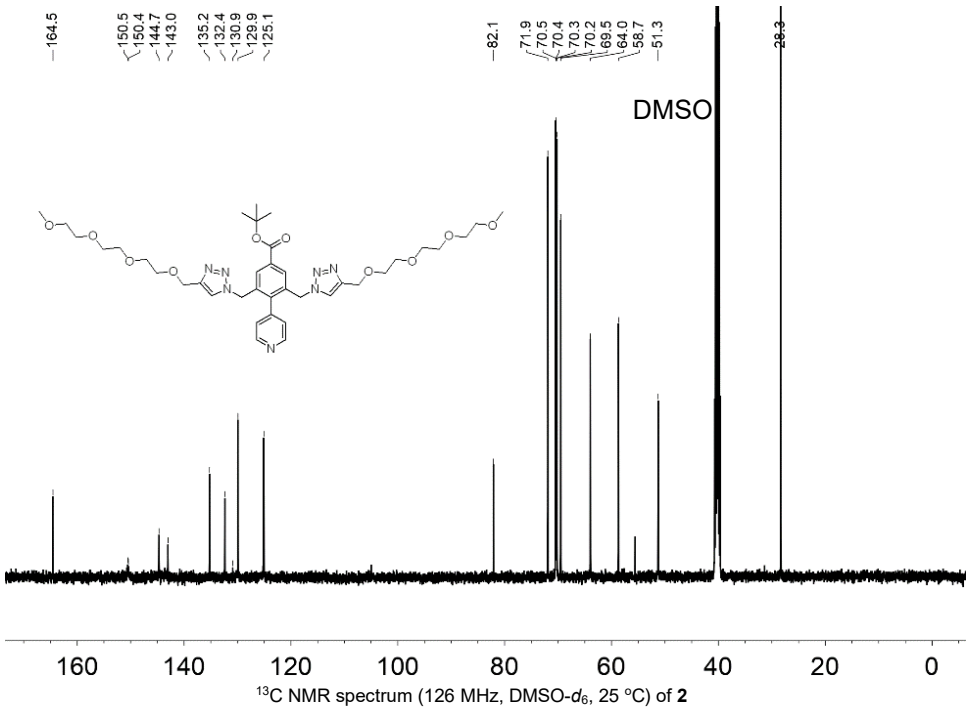

^{13}C NMR spectrum (126 MHz, DMSO-d_6, 25 °C) of **2**

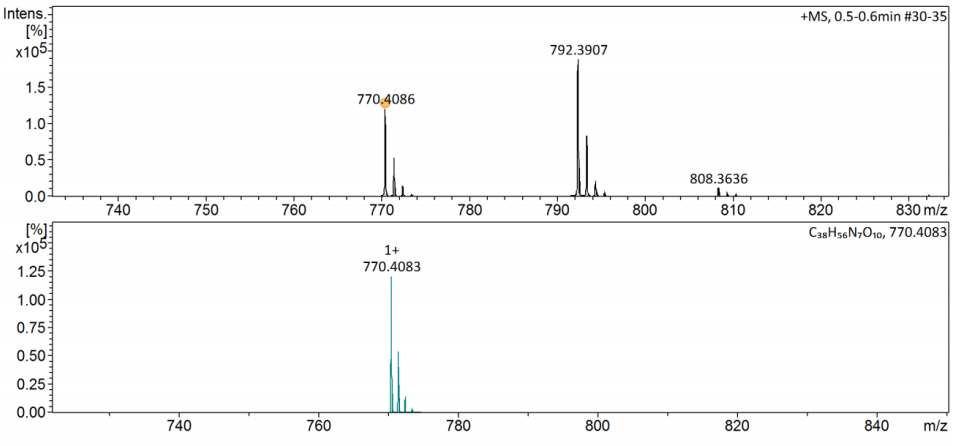

Meas. m/z	#	Ion Formula	m/z	err [ppm]	Mean err [ppm]	rdb	N-Rule	e⁻ Conf
770.408558	1	C38H56N7O10	770.408317	-0.3	-0.0	14.5	ok	even

HRMS (ESI-TOF) spectrum of **2**

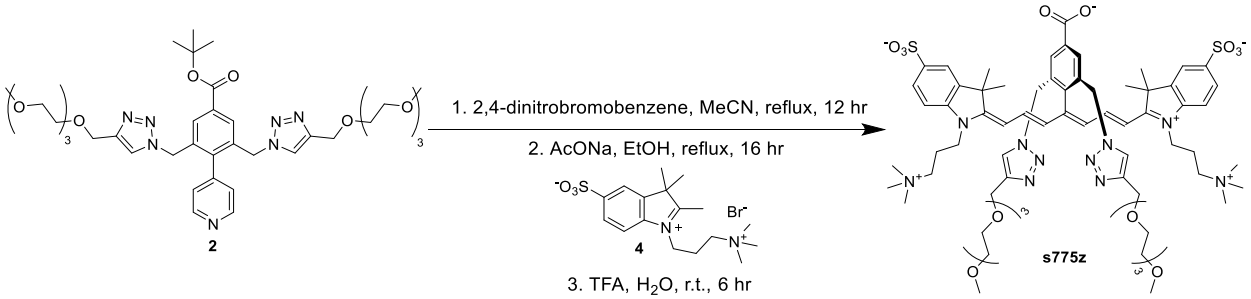

A mixture of **2** (100 mg, 130 µmol, 1 eq) and 2,4-dinitrobromobenzene (128 mg, 520 µmol, 4 eq) in MeCN (10 mL) was refluxed for 12 hr under argon atmosphere. Solvent was removed under reduced pressure, and the residue was transferred into a 20 mL centrifuge tube. Diethyl ether (15 mL) was added and the mixture was sonicated for 1 min and then centrifuged at 3600 rpm for 5 min. The supernatant was discarded, and this step was repeated twice to remove the excess 2,4-dinitrobromobenzene. The brown oil was collected and dried to afford the Zincke salt. A solution of the Zincke salt, **4** (~80 wt%, 163 mg, 390 µmol, 3 eq) and AcONa (63.9 mg, 779 µmol, 6 eq) in ethanol (20 mL) was refluxed for 16 hr in the dark under argon atmosphere. EtOH was removed under reduced pressure, the residue was suspended in acetone (20 mL), sonicated and filtered to remove nonpolar impurities. The filter cake was further purified by reverse phase column chromatography (C18, 0-35% MeOH contains 0.5% TFA in H_2O) to afford the *t*Bu protected dye. The protected dye was dissolved in a mixture of water (0.1 mL) and TFA (1.9 mL), the solution was stirred at r.t. for 6 hr in the dark. TFA and water were removed under reduced pressure, the residue was washed with acetone and dried to afford **s775z** as a dark green solid (55 mg, 31%). ^{1}H NMR (500 MHz, D_2O, 25 °C) δ (ppm): 8.62 (s, 2H), 8.11 (s, 2H), 7.85 (d, *J* = 8.0 Hz, 2H), 7.78 (s, 2H), 7.38 (d, *J* = 8.0 Hz, 2H), 6.81 (d, *J* = 13.5 Hz, 2H), 6.73 (dd, *J* = 13.5, 13.5 Hz, 2H), 6.34 (d, *J* = 13.5 Hz, 2H), 5.61 (s, 4H), 4.46 (s, 4H), 4.21 (br s, 4H), 3.60-3.36 (m, 28H), 3.33 (s, 6H), 3.18 (s, 18H), 2.32 (br s, 4H), 1.14 (s, 12H). ^{13}C NMR (126 MHz, D_2O, 25 °C) δ (ppm): 173.2, 168.0, 147.8, 143.9, 143.6, 141.6, 141.4, 140.2, 134.3, 133.0, 132.4, 126.9, 125.8, 120.0, 117.5, 115.2, 112.8, 111.0, 71.1, 69.6, 69.5, 69.4, 69.1, 63.2, 62.9, 58.1, 53.2, 51.2, 48.8, 41.0, 27.3, 21.0 (including one overlapped aliphatic peak). HRMS (ESI-TOF) m/z: $[M + 2H]^{2+}$ calcd for $C_{68}H_{98}N_{10}O_{16}S_2^{2+}$ 687.3296, found 687.3292.

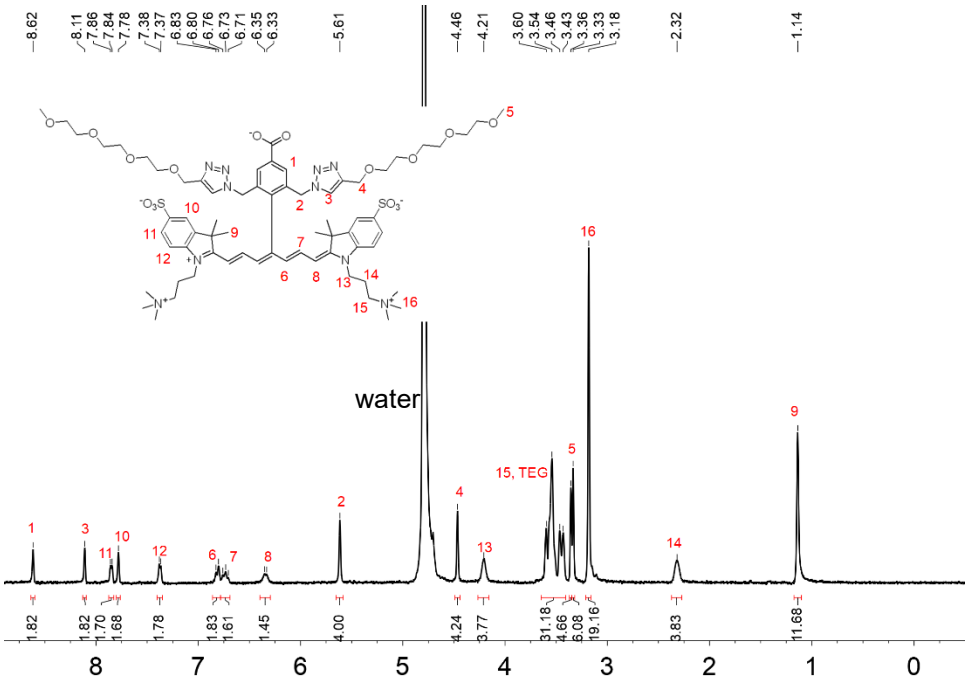

^{1}H NMR spectrum (500 MHz, D_2O, 25 °C) of **s775z**

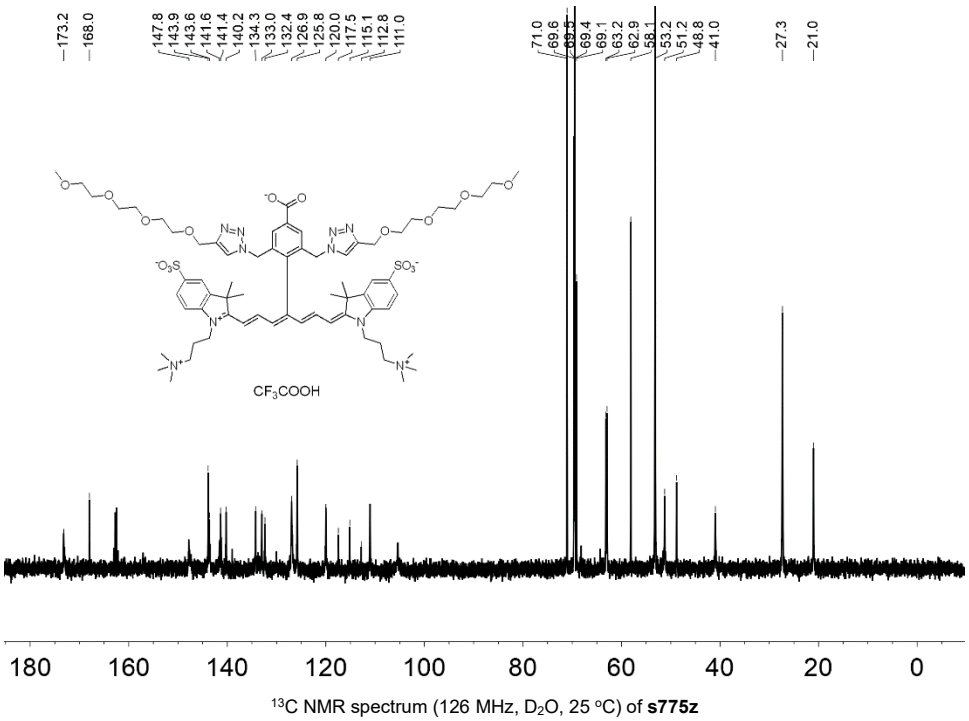

^{13}C NMR spectrum (126 MHz, D_2O, 25 °C) of **s775z**

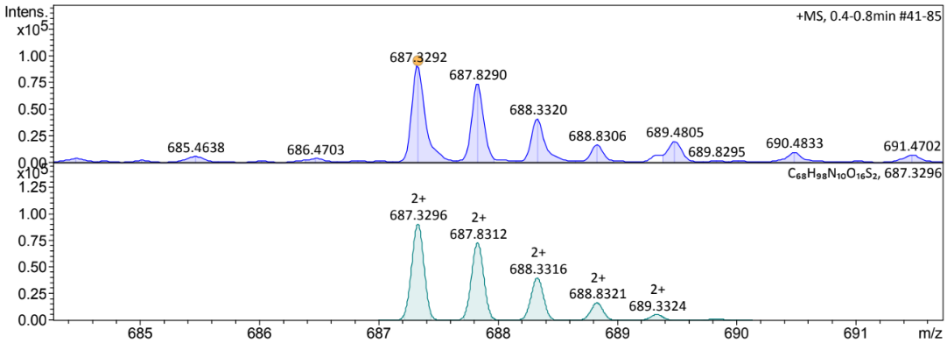

Meas. m/z	#	Ion Formula	m/z	err [ppm]	mSigma	# mSigma	Score	rdb	e¯ Conf	N-Rule
687.3292	1	C68H98N10O16S2	687.3296	0.6	25.9	1	100.00	25.0	even	ok

HRMS (ESI-TOF) spectrum of **s775z**

Synthesis of **C800-SO$_3$** by the Ring-Opening of a Zincke salt [2,3]

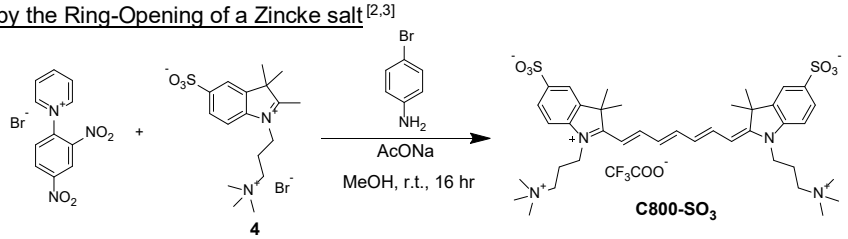

To a solution of the pyridine Zincke salt (200 mg, 613 µmol, 1 eq) in MeOH (10 mL) was added 4-bromoaniline (127 mg, 736 µmol, 1.2 eq), the resultant brown solution was stirred at r.t. for 30 min. Then **4** (~80 wt%, 965 mg, 1.84 mmol, 3 eq) and AcONa (302 mg, 3.68 mmol, 6 eq) were added. The solution was stirred at r.t. for 16 hr in the dark. MeOH was removed under reduced pressure, the residue was suspended in ethyl acetate (20 mL), sonicated and filtered to remove nonpolar impurities. The filter cake was further purified by reverse phase column chromatography (C18, 0-40% MeOH contains 0.5% TFA in H_2O) to afford **C800-SO$_3$** (55 mg, 11%) as a green solid. ^{1}H NMR (500 MHz, D_2O, 25 °C) δ (ppm): 7.99 (dd, *J* = 13.0, 13.0 Hz, 2H), 7.85 (s, 2H), 7.80 (d, *J* = 8.4 Hz, 2H), 7.58 (t, *J* = 13.0 Hz, 1H), 7.28 (d, *J* = 8.4 Hz, 2H), 6.58 (t, *J* = 13.0 Hz, 2H), 6.29 (d, *J* = 13.4 Hz, 2H), 4.16 (t, *J* = 7.0 Hz, 4H), 3.45 (t, *J* = 8.0 Hz, 4H), 3.09, (s, 18H), 2.30 (tt, *J* = 8.0, 7.0 Hz, 4H), 1.60 (s, 12H).

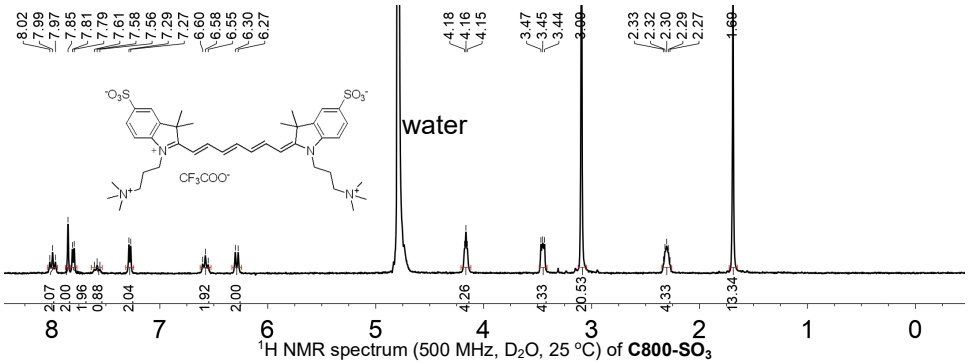

^{1}H NMR spectrum (500 MHz, D_2O, 25 °C) of **C800-SO$_3$**

Modified Synthesis of Literature Dyes **ZWCl** and **756z** [4,5]

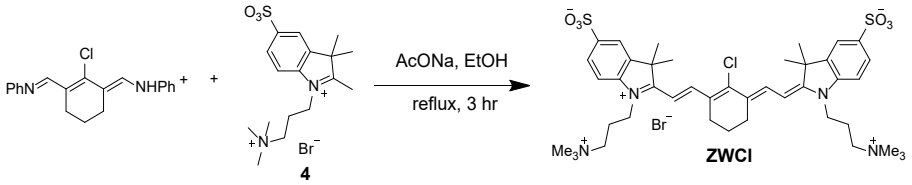

A mixture of aniline protected Vilsmeier reagent (300 mg, 929 µmol, 1 eq), **4** (~80 wt%, 1.38 g, 2.04 mmol, 2.2 eq), and AcONa (153 mg, 1.86 mmol, 2 eq) in absolute EtOH (20 mL) was refluxed for 3 hr under argon atmosphere in the dark. The reaction was cooled to room temperature, Et_2O (100 mL) was added and the mixture was filtered. The solid was washed with MeOH to afford **ZWCl** as a green solid (620 mg, 75%). ^{1}H NMR (500 MHz, D_2O, 25 °C) δ (ppm): 8.36 (d, *J* = 13.9 Hz, 2H), 7.89 (s, 2H), 7.78 (d, *J* = 8.1 Hz, 2H), 7.29 (d, *J* = 8.4 Hz, 2H), 6.24 (d, *J* = 13.9 Hz, 2H), 4.24 (br s, 4H), 3.50 (br s, 4H), 3.12 (s, 18H), 2.56 (br s, 4H), 2.34 (br s, 4H), 1.73 (m, 14H).

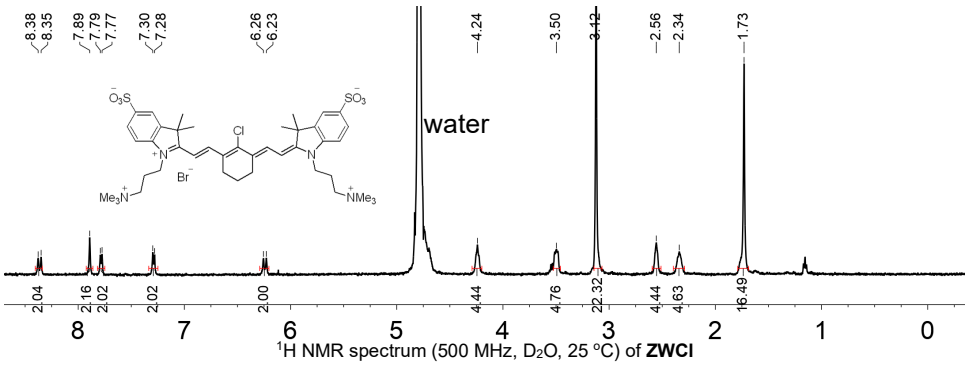

^{1}H NMR spectrum (500 MHz, D_2O, 25 °C) of **ZWCl**

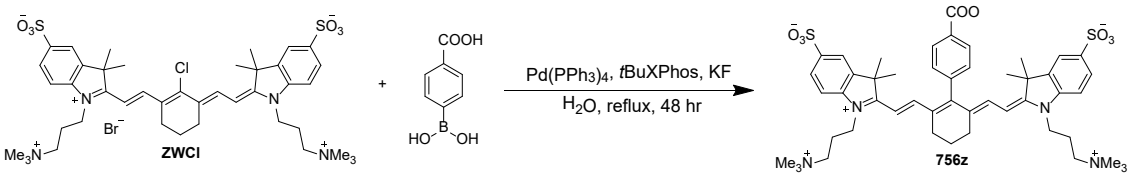

A mixture of **ZWCl** (100 mg, 112 µmol, 1 eq), 4-carboxyphenylboric acid (92.8 mg, 559 µmol, 5 eq), $Pd(PPh_3)_4$ (6.46 mg, 5.59 µmol, 5 mol%), *t*BuXPhos (4.75 mg, 11.2 µmol, 10 mol%) and KF (32.5 mg, 559 µmol, 5 eq) in H_2O (10 mL) was refluxed for 48 hr under argon atmosphere in the dark. The reaction was monitored by absorption spectroscopy (maximum absorption changed from 777 nm to 756 nm). The reaction was cooled to room temperature and extracted by ethyl acetate (3 × 10 mL) to remove nonpolar impurities. The aqueous phase was purified by reverse phase column chromatography (C18, 0-40% MeOH contains 0.5% TFA in H_2O) to afford **756z** (47 mg, 47%) as a green solid. ^{1}H NMR (500 MHz, DMSO-d_6, 25 °C) δ (ppm): 8.22 (d, *J* = 7.8 Hz, 2H), 7.64 (s, 2H), 7.61 (d, *J* = 8.2 Hz, 2H), 7.36 (d, *J* = 7.8 Hz, 2H), 7.31 (d, *J* = 8.2 Hz, 2H), 7.05 (d, *J* = 13.7 Hz, 2H), 6.23 (d, *J* = 13.7 Hz, 2H), 4.15 (br s, 4H), 3.04 (s, 18H), 2.72 (br s, 4H), 2.09 (br s, 4H), 1.95 (br s, 4H), 1.57 (br s, 2H), 1.12 (s, 12H).

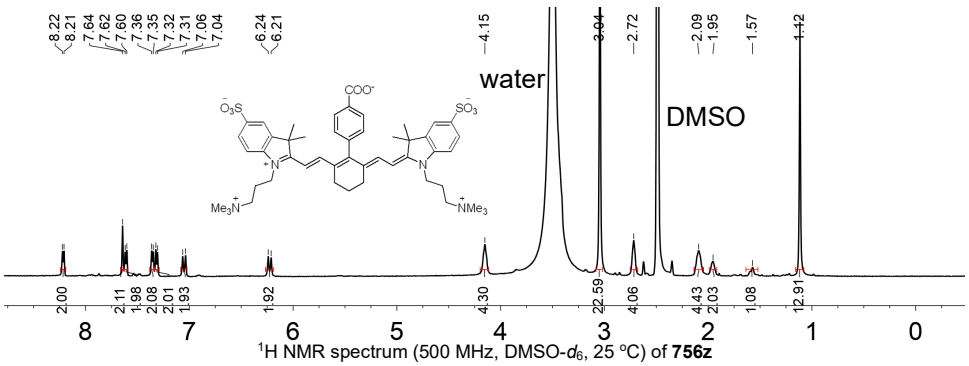

^{1}H NMR spectrum (500 MHz, DMSO-d_6, 25 °C) of **756z**

Synthesis of Literature Dye **UL766** [6]

Compound **UL766** was prepared by a literature method.[6] ^{1}H NMR (500 MHz, D_2O, 25 °C) δ (ppm): 8.09 (d, *J* = 14.0 Hz, 2H), 7.88 (s, 2H), 7.84 (d, *J* = 8.1 Hz, 2H), 7.37 (d, *J* = 8.1 Hz, 2H), 6.33 (d, *J* = 14.0 Hz, 2H), 4.38 (br s, 4H), 4.23 (br s, 2H), 3.98 (br s, 4H), 3.76 (m, 2H), 3.63 (br s, 4H), 3.55 (br s, 4H), 3.44 (br s, 4H), 3.39 (br s, 4H), 3.31 (s, 9H), 3.27 (s, 6H), 2.62 (br s, 4H), 2.53 (br s, 2H), 1.89 (br s, 2H), 1.77 (s, 12H).

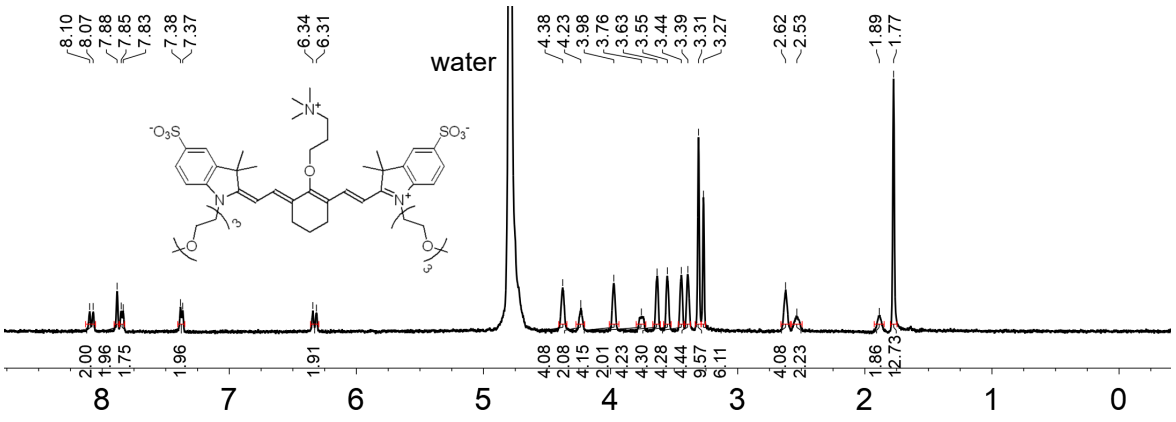

^{1}H NMR spectrum (500 MHz, D_2O, 25 °C) of **UL766**

3. Solubility Differences

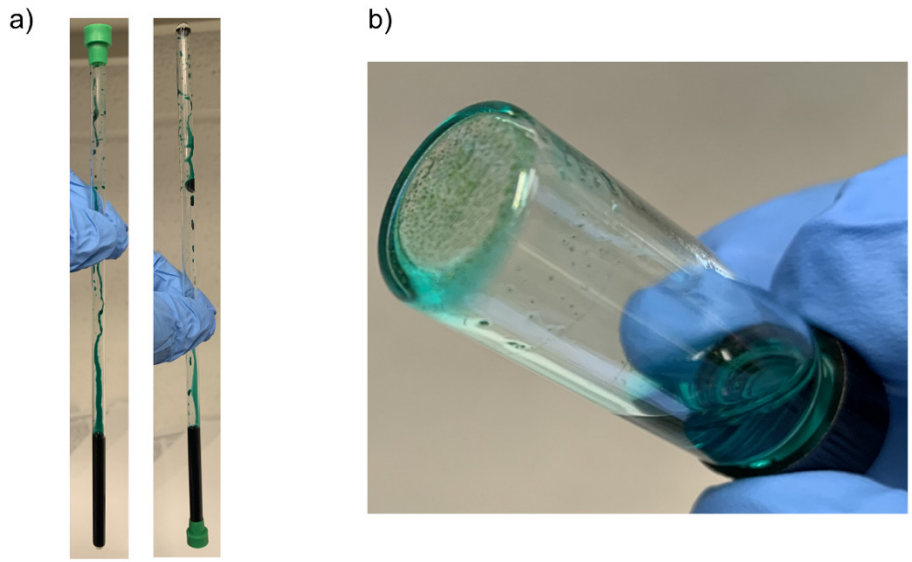

Figure S1. a) NMR tube containing 100 mM **s775z** in D_2O. The NMR peaks are sharp and there is no insoluble material in the NMR tube, indicating the dye has high solubility in water. b) A vial showing that a freshly prepared 1 mM stock solution of **756z** in H_2O forms a precipitate after 24 hours, and the insoluble material cannot be redissolved after sonication.

4. NMR Spectra of s775z and Related Dyes

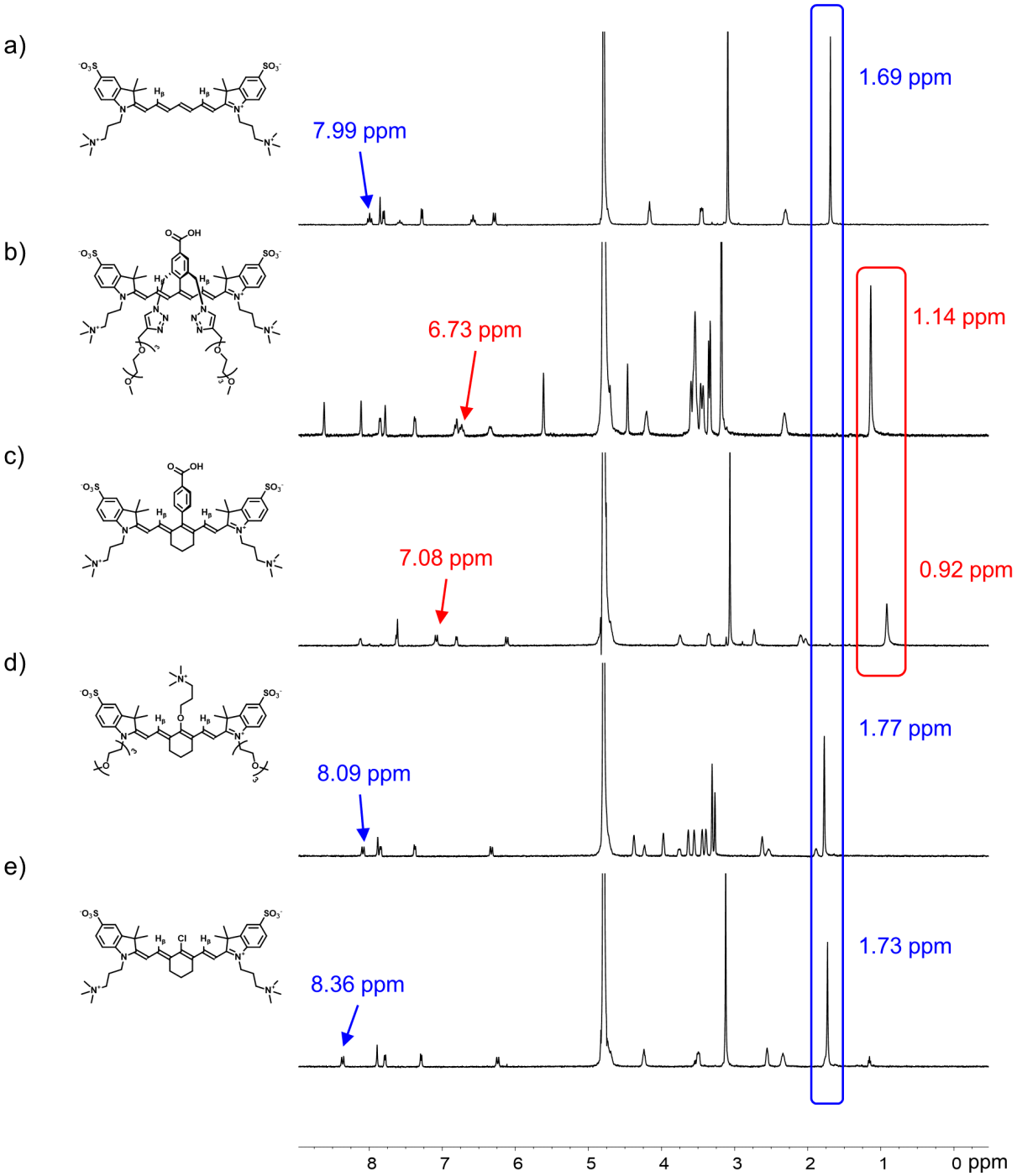

Figure S2. ^{1}H NMR spectra (500 MHz, D_2O, 25 °C) of a) **C800-SO$_3$**, b) **s775z**, c) **756z**, d) **UL766** and e) **ZWCl**. The upfield chemical shift of the indolenine gem-dimethyl protons (highlighted by red and blue rectangles) and H_β (highlighted by red and blue arrows) in **756z** and **s775z** is due to strong shielding by the face of the rotated meso-Aryl ring.

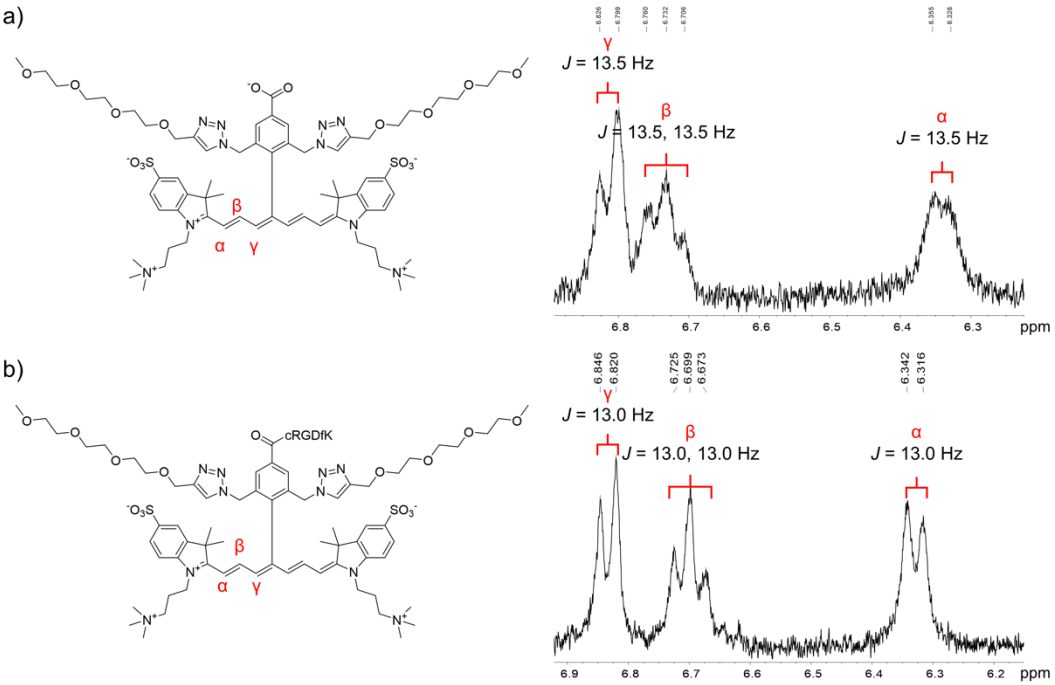

Figure S3. Partial ^{1}H NMR spectrum (500 MHz, D_2O, 25 ºC) of a) **s775z** and b) **s775z-RGD**. The three polyene protons exhibit large $^{3}J_{HH}$ coupling constants indicating all-*trans* double bonds. Typically, $^{3}J_{HH}$ is ~10 Hz for a *cis* double bond.

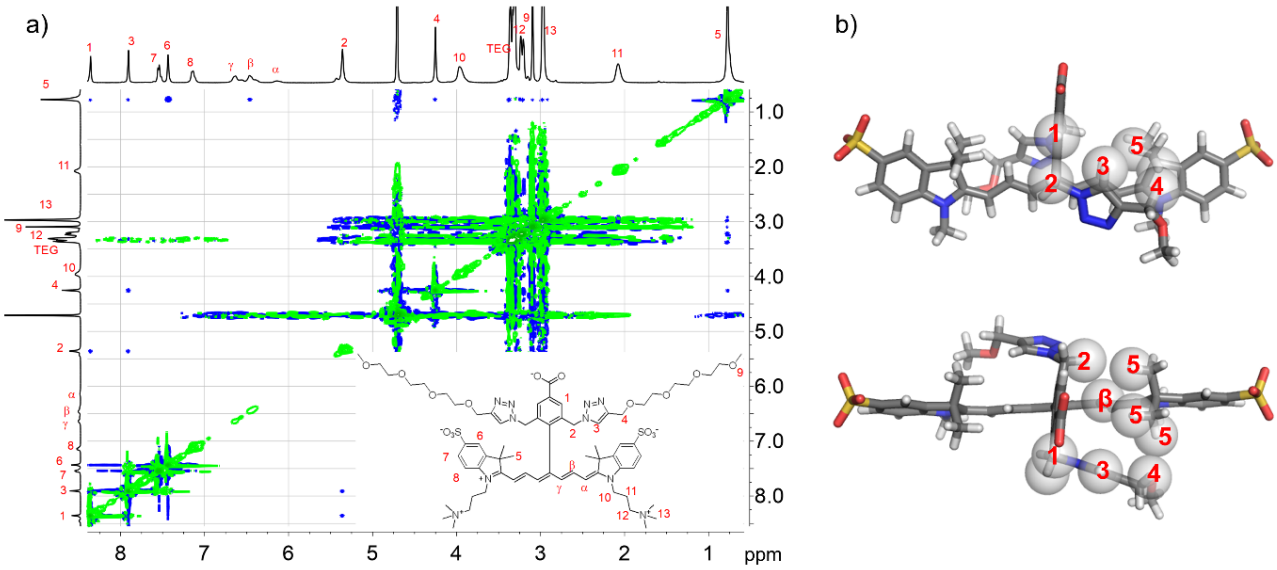

Figure S4. a) ^{1}H-^{1}H ROESY NMR spectrum (500 MHz, D_2O, 25 ºC) of **s775z**. b) Molecular model of **s775z** that explains the observed cross peaks between indolenine gem-dimethyl protons 5 and heptamethine polyene protons β, as well as shielding chain protons 1, 3 and 4. Solubilizing chains in the model were abbreviated to methyl groups for viewing clarity.

5. Bioconjugation

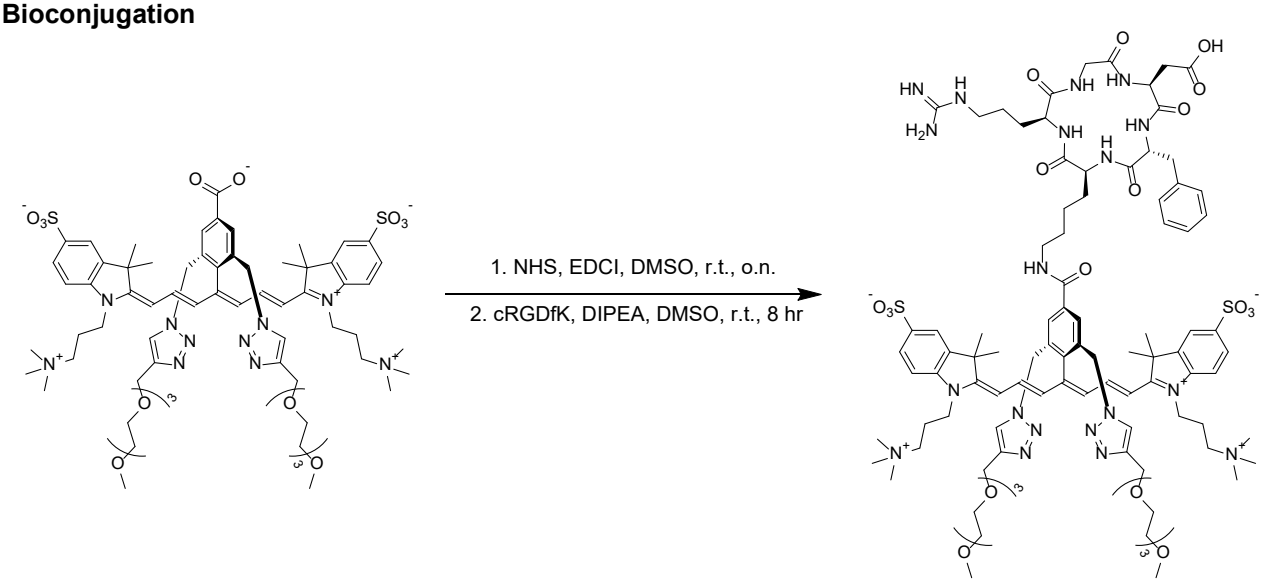

s775z-RGD: A mixture of the **s775z** (10.0 mg, 8.35 μmol, 1 eq), N-hydroxysuccinimide (2.88 mg, 25.1 μmol, 3 eq) and N-(3-dimethylaminopropyl)-N′-ethylcarbodiimide hydrochloride (4.80 mg, 25.1 μmol, 3 eq) in DMSO (1 mL) in a 20 mL centrifuge tube was shaken at r.t. overnight. Ethyl acetate (15 mL) was added to the tube and mixture was sonicated for 1 min and then centrifuged at 3600 rpm for 5 min. The supernatant was discarded and the green solid was washed with ethyl acetate (2 x 15 mL) and diethyl ether (1 x 15 mL); then dried to afford **s775z** NHS ester which was used without further purification and could be stored at -30 °C for a month. A mixture of crude **s775z** NHS ester (8.35 μmol, 1 eq), cRGDfK (10.1 mg, 16.7 μmol, 2 eq) and DIPEA (6.90 μL, 41.8 μmol, 5 eq) in DMSO (0.5 mL) was stirred at room temperature for 8 hr. The mixture was directly purified by reverse phase column chromatography (C18, 0-35% MeOH contains 0.5% TFA in H_2O) to afford **s775z-RGD** as green solid (8 mg, 54%). The structure and high purity were confirmed by ^{1}H NMR, mass spectrometry and HPLC analysis. ^{1}H NMR (500 MHz, D_2O, 25 °C) δ (ppm): 8.40 (s, 2H), 7.95 (s, 2H), 6.87 (d, *J* = 8.5 Hz, 2H), 7.49 (s, 2H), 7.21 (d, *J* = 8.5 Hz, 2H), 7.06 – 6.99 (m, 5H), 6.72 (d, *J* = 13.0 Hz, 2H), 6.59 (dd, *J* = 13.0, 13.0 Hz, 2H), 6.22 (d, *J* = 13.0 Hz, 2H), 5.48 (s, 4H), 4.30 – 4.26 (m, 6H), 4.11 – 4.06 (m, 6H), 3.71 (d, *J* = 9.0 Hz, 1H), 3.41 – 3.23 (m, 31H), 3.17 (s, 6H), 3.02 – 2.93 (m, 20 H), 2.84 – 2.79 (m, 1H), 2.75 – 2.70 (m, 1H), 2.75 – 2.52 (m, 1H), 2.17 (m, 5H), 1.74 (br s, 1H), 1.59 (br s, 1H), 1.53 (br s, 1H), 1.40 (m, 6H), 0.89 –0.77 (m, 16H). HRMS (ESI-TOF) m/z: $[M]^+$ calcd for $C_{95}H_{136}N_{19}O_{22}S_2^+$ 1958.9543, found $[M]^+$ 1958.9588.

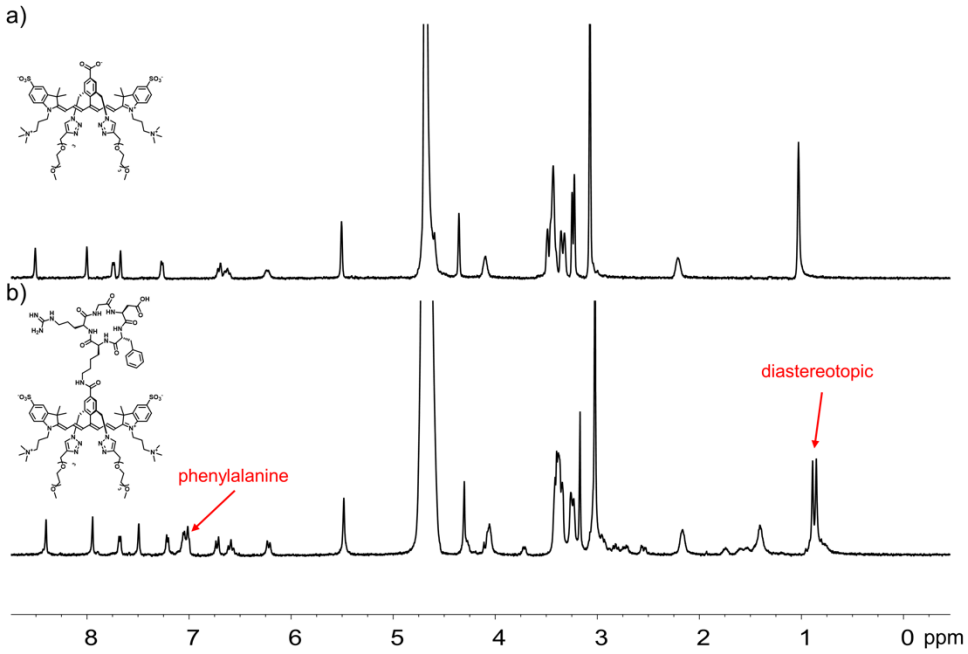

Figure S5. ^{1}H NMR spectra (500 MHz, D_2O, 25 °C) of a) **s775z** and b) **s775z-RGD**. Phenylalanine protons of cRGDfK is indicated. The indolenine gem-dimethyl groups of **s775z-RGD** are diastereotopic due to the attachment of chiral cRGDfK peptide. All the NMR peaks for **s775z-RGD** are relatively sharp indicating little or no self-aggregation at the 1 mM NMR concentration.

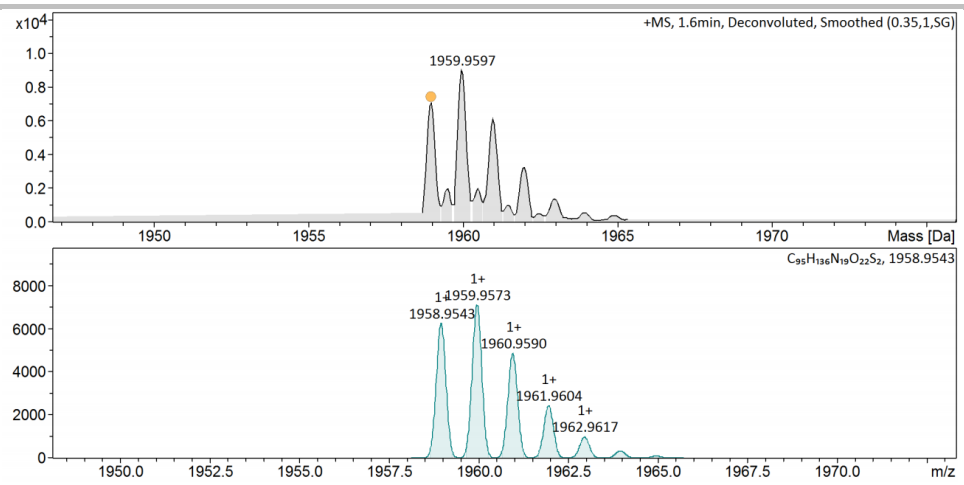

Meas. m/z	#	Ion Formula	m/z	err [ppm]	Mean err [ppm]	rdb	N-Rule	e⁻ Conf
1958.958794	1	C95H136N19O22S2	1958.954326	-2.3	491.1	37.5	ok	even

HRMS (ESI-TOF) spectrum of **s775z-RGD**

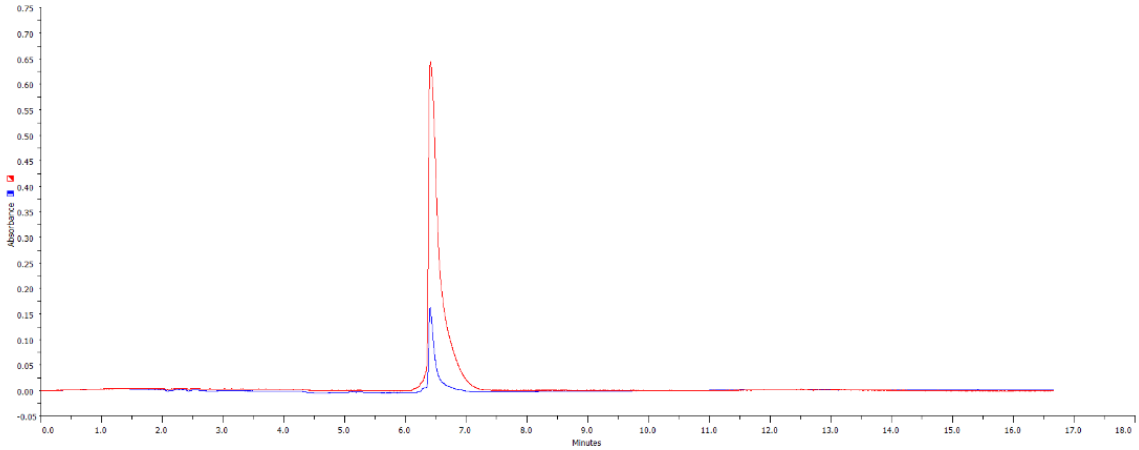

HPLC spectrum of **s775z-RGD** showing high purity. Solvent: 0-95% acetonitrile in water with 0.1% TFA; flow rate: 1 mL/min; detector: 750 nm (red) and 260 nm (blue). Retention time = 6.42 min.

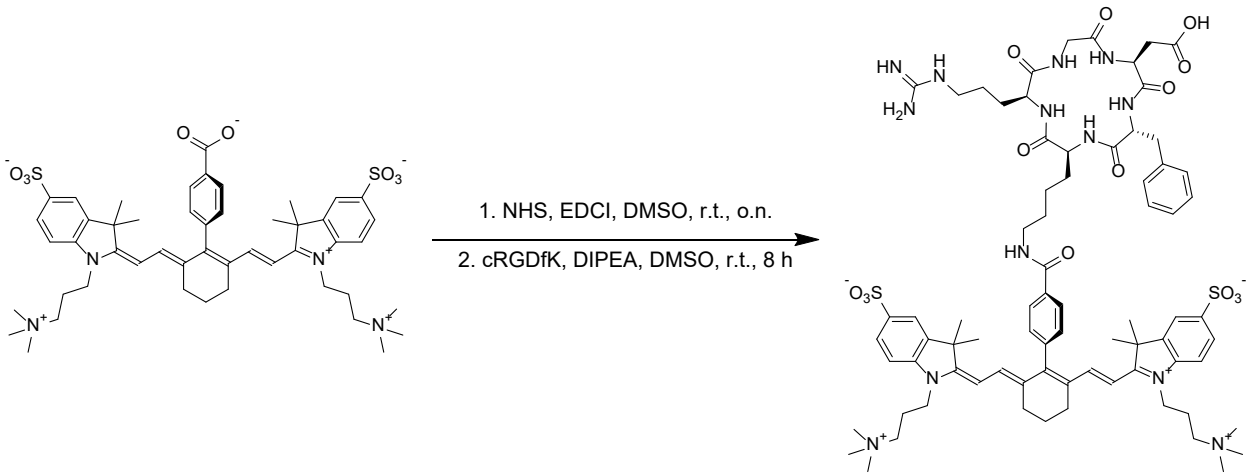

Compound **756z-RGD** was synthesized by using the same amide bond coupling procedure described above. Reverse phase column chromatography: C18, 0-50% MeOH contains 0.5% TFA in H_2O. The structure and high purity were confirmed by ^1H NMR, mass spectrometry and HPLC analysis. HRMS (ESI-TOF) m/z: $[M]^+$ calcd for $C_{76}H_{103}N_{13}O_{14}S_2^+$ 1485.7183, found $[M]^+$ 1485.7187. Many of the NMR peaks were broad because of self-aggregation in water but diagnostics peaks were present.

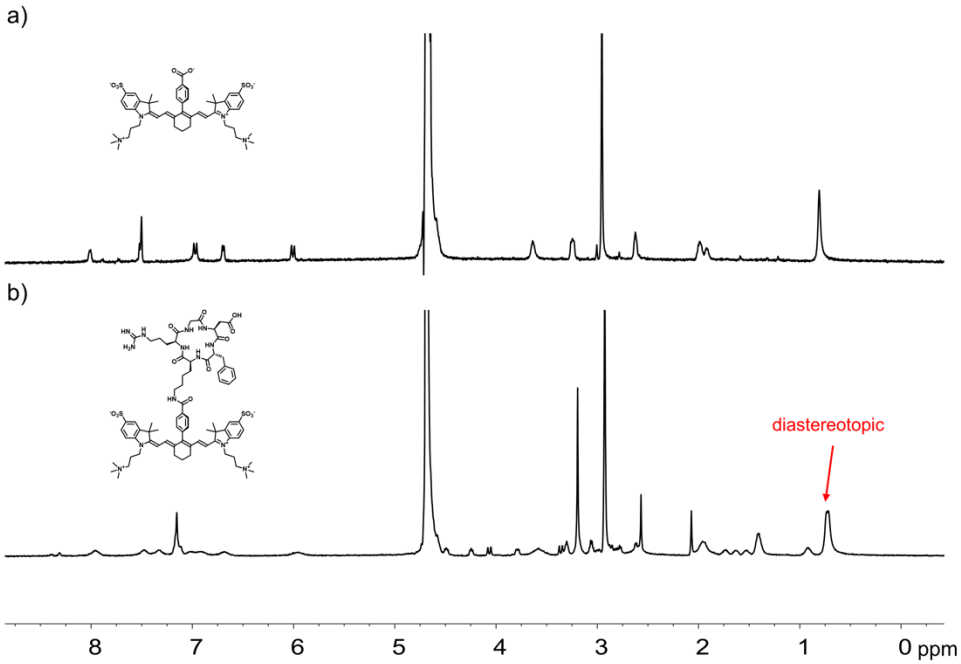

Figure S6. ^{1}H NMR spectra (500 MHz, D_2O, 25 °C) for a) **756z** and b) **756z-RGD**. The indoline gem-dimethyl groups of **756z-RGD** are diastereotopic and exhibit two peaks due to the attachment of chiral cRGDfK peptide. Most NMR peaks for **756z-RGD** are broad because of self-aggregation in water.

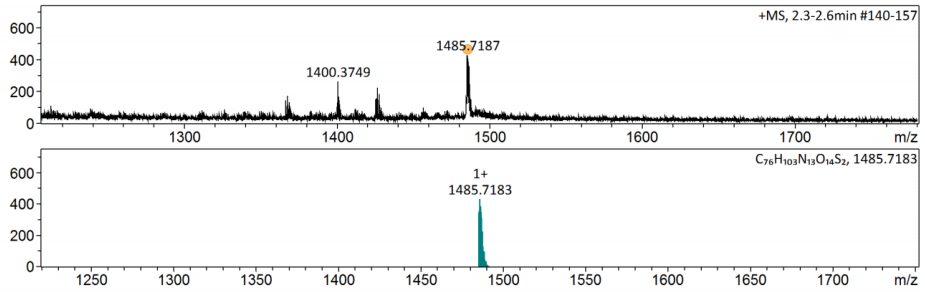

Meas. m/z	#	Ion Formula	m/z	err [ppm]	Mean err [ppm]	rdb	N-Rule	e¯ Conf
1485.718668	1	C76H103N13O14S2	1485.718338	-0.2	1252.6	32.0	ok	odd

HRMS (ESI-TOF) spectrum of **756z-RGD**

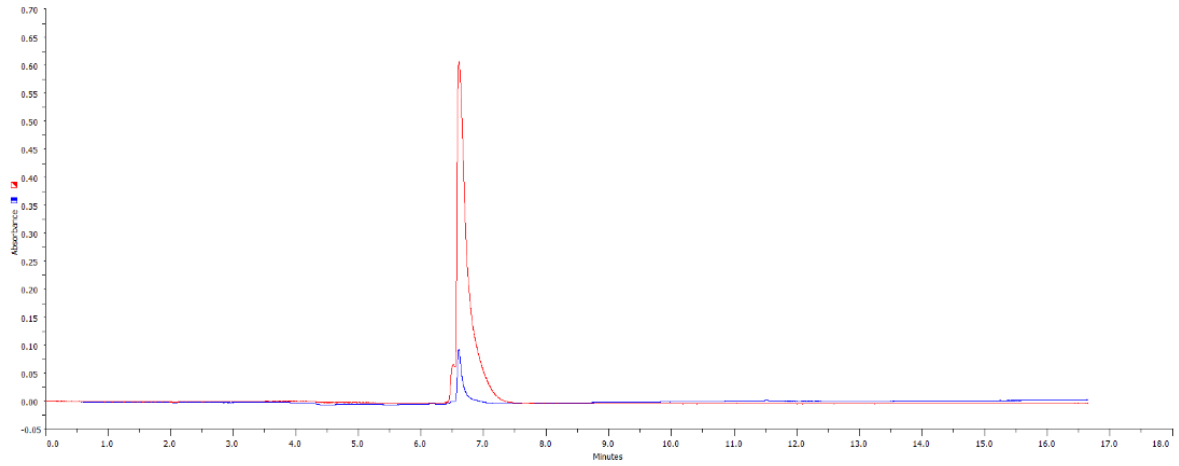

HPLC spectrum of **756z-RGD** showing high purity. Solvent: 0-95% acetonitrile in water with 0.1% TFA; flow rate: 1 mL/min; detector: 750 nm (red) and 260 nm (blue). Retention time = 6.61 min.

6. Photophysical Properties

Table S1. Spectral properties of **756z** and **s775z** and their RGD conjugates.

Dye	Solvent[a]	λ^{abs}_{max} (nm)[b]	λ^{em}_{max} (nm)	SS (nm)[c]	ε ($M^{-1}cm^{-1}$)	R^2
756z	H_2O	681 (a) / 756 (m)	773	17	56,000	0.970[d]
	PBS	681 (a) / 756 (m)	773	17	99,000	0.942[d]
	2 μM BSA	681 (a) / 755 (m)	773	18	107,000	0.986[d]
	100% FBS	682 (a) / 758 (m)	774	16	118,000	0.978[d]
s775z	H_2O	775	795	20	201,000	0.999
	PBS	775	794	19	201,000	0.999
	2 μM BSA	775	795	20	204,000	0.999
	100% FBS	776	795	19	200,000	0.999
756z-RGD	PBS	682 (a) / 757 (m)	773	16	147,000	0.998
s775Z-RGD	PBS	776	795	19	188,000	0.999

[a] PBS = Phosphate buffered saline (pH 7.4); 2 μM BSA = 2 μM solution of bovine serum albumin in pH 7.4 PBS; FBS = fetal bovine serum. Dye concentration range is 0 – 5 μM. All measurements were done at room temperature. [b] a = aggregate; m = monomer. [c] SS = Stokes shift. [d] Nonlinear relationship with concentration, caused by self-aggregation.

Quantum yield measurements used **UL766** (Φ_f = 9.5% in pH 7.4 PBS) as a reference standard.[6] The concentrations of **UL766** and other cyanine dyes were adjusted to the absorption value of 0.08 at 730 nm. The fluorescence spectrum of each solution was obtained with excitation at 730 nm, and the integrated area was used in the quantum yield calculation by the following equation:

$$\Phi_{sample} = \Phi_{ref} \times \frac{\eta^2_{sample}\ I_{sample}\ A_{sample}}{\eta^2_{ref}\ I_{ref}\ A_{ref}}$$

where η is the refractive index of the solvent, I is the integrated fluorescence intensity, and A is the absorbance at a chosen wavelength. The estimated error for this method is ±10%.

Table S2. Fluorescence brightness of various heptamethine dyes in pH 7.4 PBS.[a]

Dye	ε ($M^{-1}cm^{-1}$)	Quantum yield (%)	Fluorescence brightness[c]
s775z	201,000	9.0[b]	18,000
756z	99,000	9.7[b]	9,600
s775z-RGD	188,000	8.1[b]	15,000
756z-RGD	147,000	10.7[b]	16,000
UL766[d]	229,000	9.5	22,000
ICG	71,000	2.3[b]	1,600
ZW800-1[d]	246,000	13.5	33,000
CW800[d]	242,000	9.0	22,000

[a] All measurements were done at room temperature. [b] Relative to **UL766** in pH 7.4 PBS, error is ±10%. [c] Fluorescence brightness = ε × quantum yield, error is ±15%. [d] Literature data.[6–8]

7. Absorption, Excitation and Emission Spectra of s775z and 756z

Note for Figs S7-S10 and S12: the fluorescence emission intensities at the highest dye concentrations are decreased and red-shifted due to the strong inner filter (reabsorption) effect.

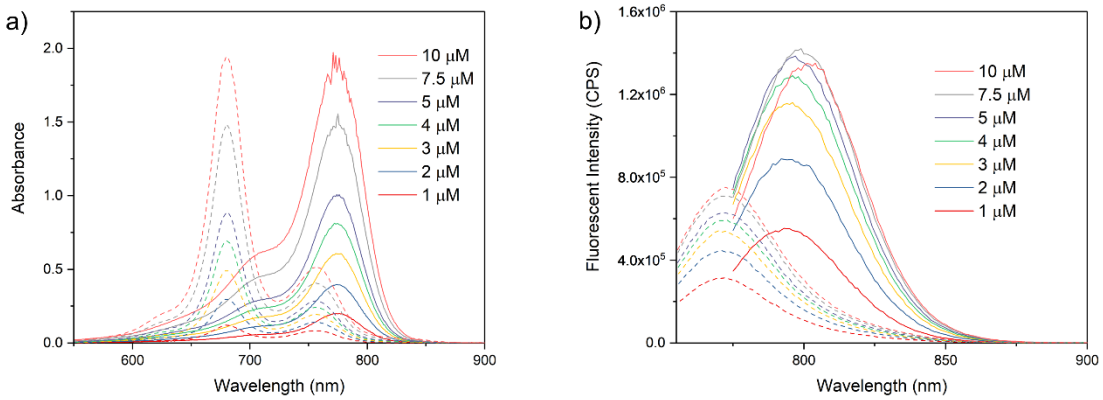

Figure S7. a) Absorption and b) emission spectra of **s775z** (solid line) and **756z** (dashed line) in water at various concentrations. For **s775z**, λ_{ex} = 765 nm. For **756z**, λ_{ex} = 745 nm.

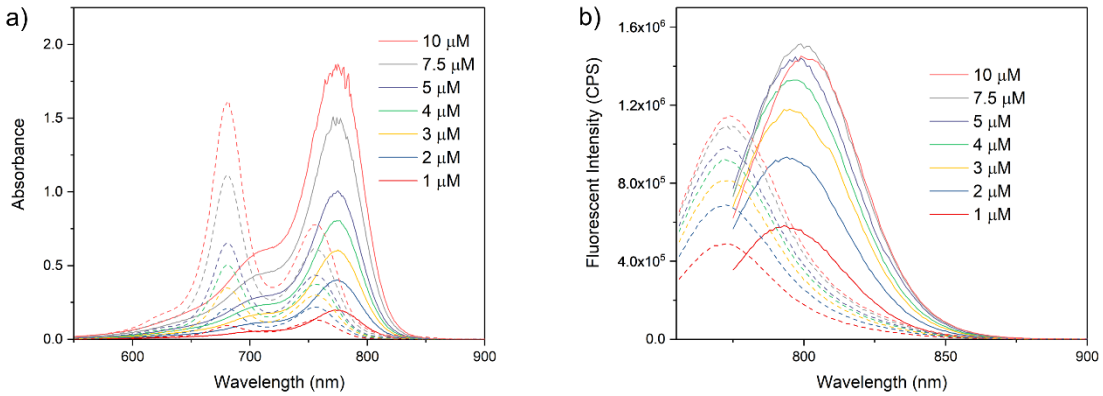

Figure S8. a) Absorption and b) emission spectra of **s775z** (solid line) and **756z** (dashed line) in PBS, pH 7.4, at various concentrations. For **s775z**, λ_{ex} = 765 nm. For **756z**, λ_{ex} = 745 nm.

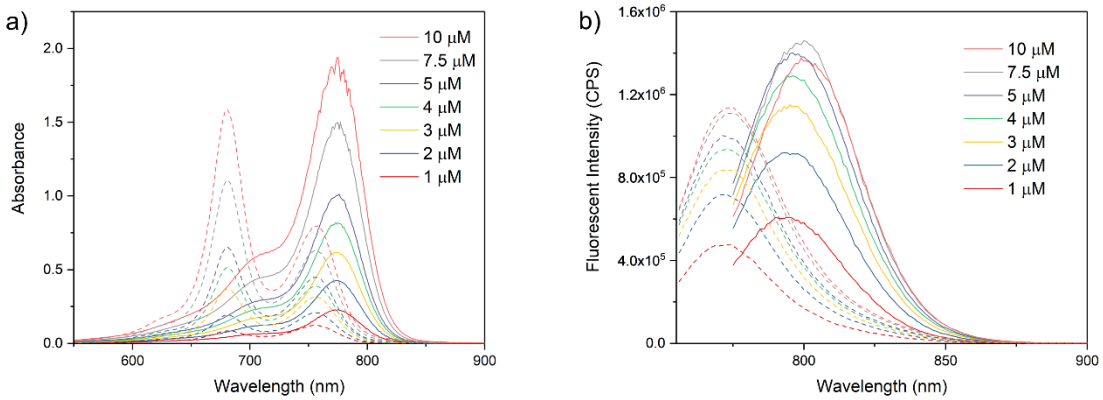

Figure S9. a) Absorption and b) emission spectra of **s775z** (solid line) and **756z** (dashed line) in 2 μM BSA at various concentrations. 2 μM BSA = 2 μM solution of bovine serum albumin in PBS, pH 7.4. For **s775z**, λ_{ex} = 765 nm. For **756z**, λ_{ex} = 745 nm.

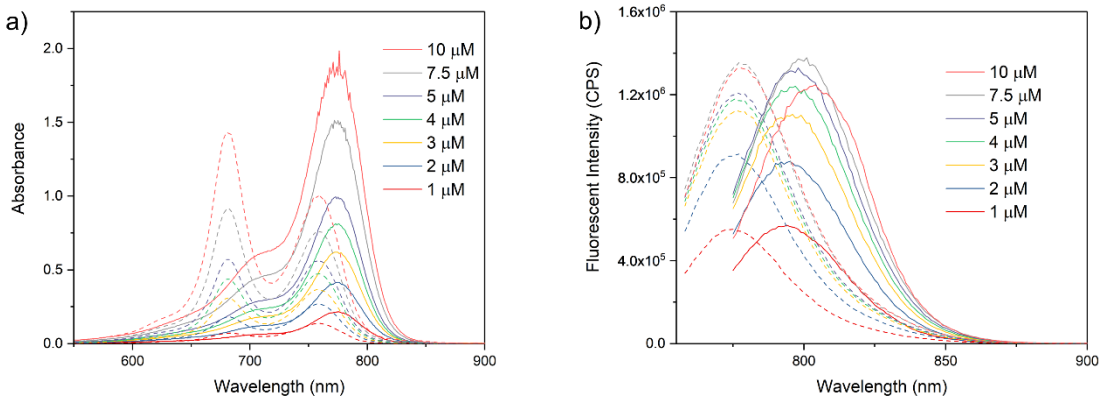

Figure S10. a) Absorption and b) emission spectra of **s775z** (solid line) and **756z** (dashed line) in 100% FBS at various concentrations. FBS = fetal bovine serum. For **s775z**, λ_{ex} = 765 nm. For **756z**, λ_{ex} = 745 nm.

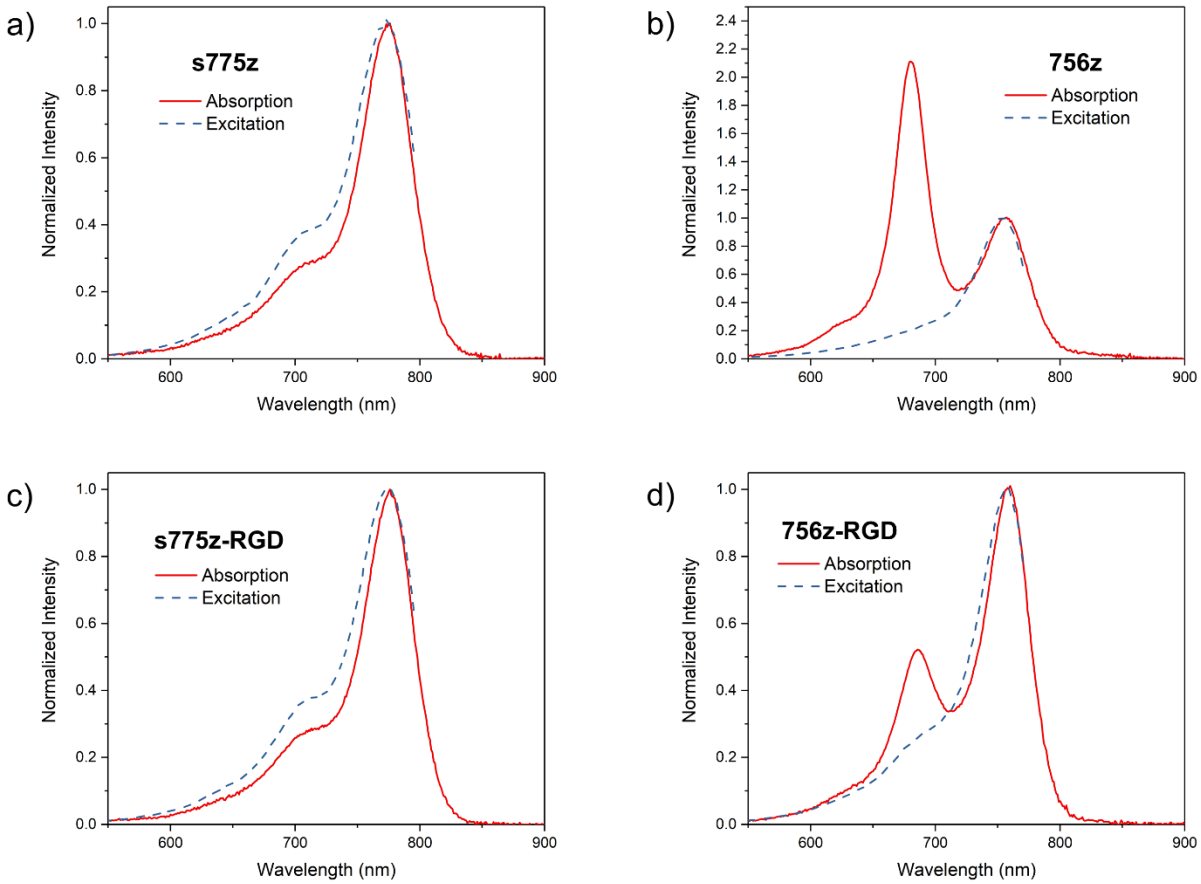

Figure S11. Absorption (red solid line) and excitation (blue dashed line) spectra of a) **s775z**, b) **756z**, c) **s775z-RGD** and d) **756z-RGD** in water (2 μM). The excitation spectra of **756z** and **756z-RGD** indicate that the H-aggregation bands are non-fluorescent. For **s775z** and **s775z-RGD**, λ_{em} = 805 nm. For **756z** and **756z-RGD**, λ_{em} = 780 nm.

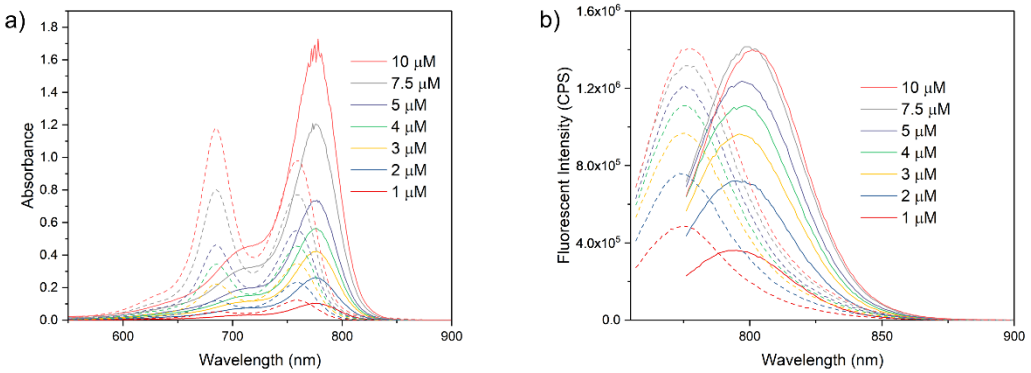

Figure S12. a) Absorption and b) emission spectra of **s775z-RGD** (solid line) and **756-RGD** (dashed line) in water at various concentrations. For **s775z-RGD**, λ_{ex} = 765 nm. For **756-RGD**, λ_{ex} = 745 nm.

8. Chemical Stability, pH Independence, and Albumin Binding

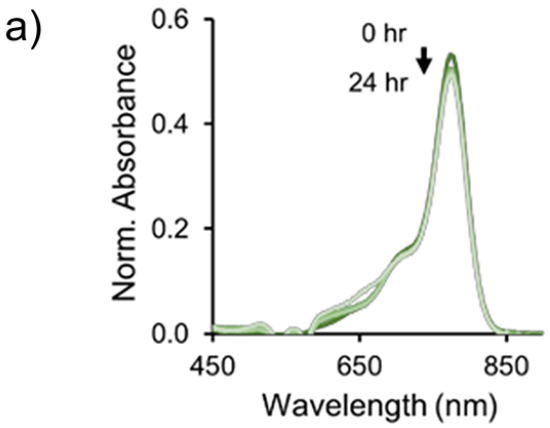

Incubation Time (hr)	0	2.5	4	6	8	24
% Dye Remaining	100%	94%	95%	95%	93%	93%

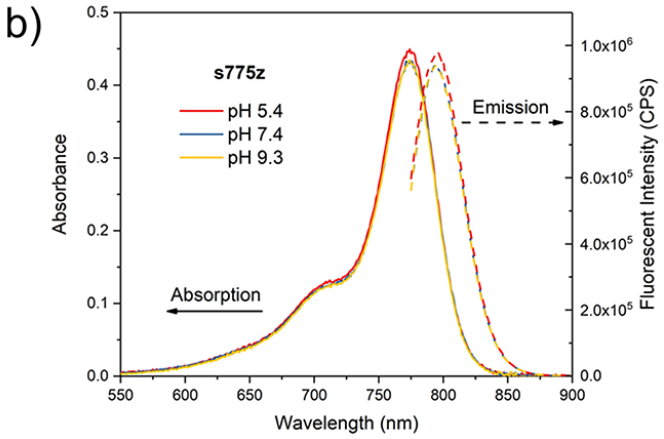

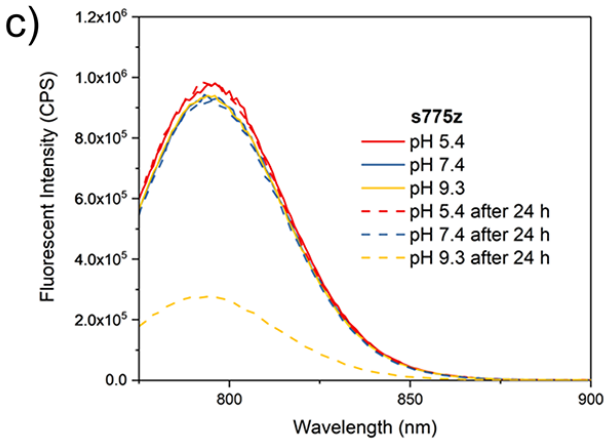

Figure S13. a) Negligible change in absorbance for shielded heptamethine **s775z** (2 μM) in 100% fetal bovine serum after 24 hr at 37 °C, pH 7.4. b) No change in absorbance/emission profile for **s775z** (2 μM) across the pH range of 5-9. c) No change in fluorescence for **s775z** (2 μM) after 24 hr at pH 5-7.

SUPPORTING INFORMATION

Albumin Binding Measurements

Two separate sets of titration experiments were performed. The first set of titration experiments measured quenching of bovine serum albumin (BSA) tryptophan fluorescence as dye was added incrementally.[9] A fluorescence spectrum (ex: 280 nm, slit width: 2 nm) was acquired after each dye aliquot was added (4 µL of a 1 mM stock solution of **s775z** or **756z**). After each aliquot addition, the solution was mixed and allowed to equilibrate for 5 min before spectral acquisition. The data is shown in Figure S14(a)-(d) and indicate weak dye/BSA affinity.

The second set of titration experiments measured the fluorescence intensity for samples of **756z** and **s775z** at different concentrations in the presence and absence of BSA (2 µM). The data in Figure S14(e)-(f) shows that the presence of the BSA had no effect on the dye fluorescence, thus indicating weak dye/BSA affinity.

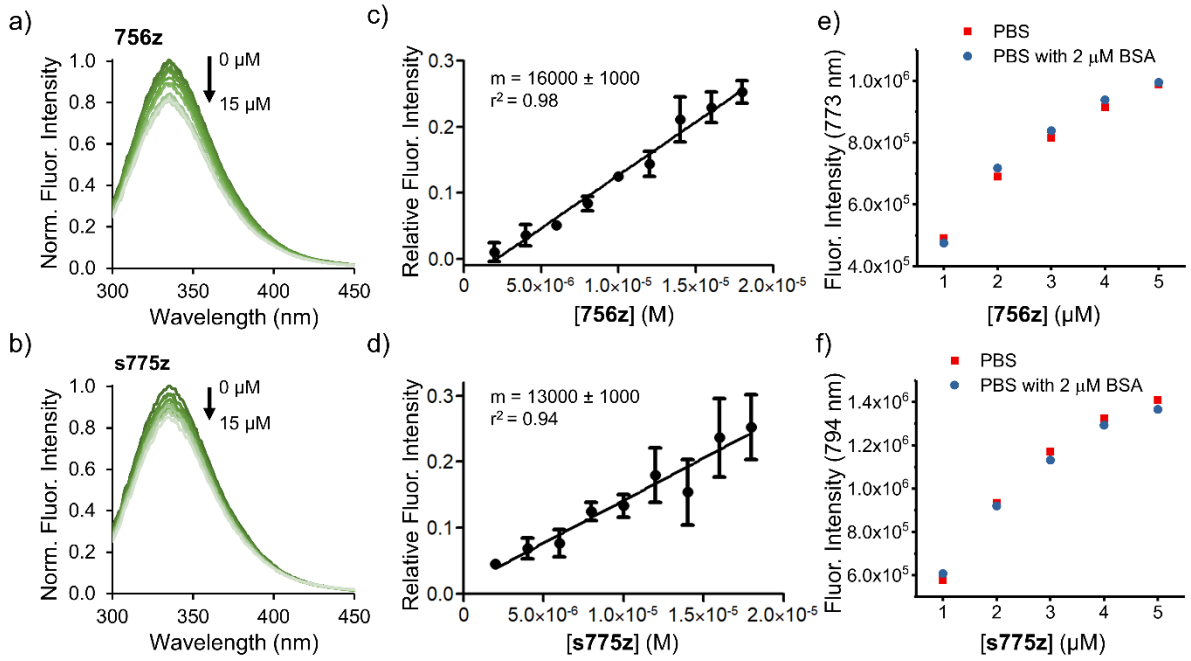

Figure S14. Aliquots of **756z** and **s775z** were added incrementally (up to 15 µM) to a solution of bovine serum albumin (BSA, 2 µM) at 37 °C. The BSA tryptophan fluorescence intensity (ex: 280 nm, slit width: 2 nm) was plotted as a function of dye concentration for a), c) **756z** and b), d) **s775z**. The relative fluorescence intensity at 335 nm was determined using the following equation, where F_0 is the initial fluorescence intensity, F is the fluorescence intensity after each aliquot addition of dye, and the slope of the trend line (m) corresponds to K_a ± SD.

$$\text{Relative Fluorescence Intensity} = \frac{F_0 - F}{F}$$

Graph of fluorescence intensity for e) **756z** (ex: 745 nm, em: 773 nm) and f) **s775z** (ex: 765 nm, em: 794 nm) in PBS at various concentrations, in the presence and absence of BSA (2 µM).

9. Photostability Measurements

Lamp Irradiation

A solution of dye (1 μM) in PBS buffer, pH 7.4, was placed in a 1x1x4 cm^3 cuvette that was exposed to air and irradiated at a distance of 3 cm by a 150 W Xenon lamp with a 620 nm long-pass filter. An absorbance spectrum was recorded every 10 min. The normalized maximum absorbance of dye was plotted against time and fitted to a non-linear regression, one-phase exponential decay. The competitive irradiation experiment used TLC analysis to track changes in a mixed solution of **s775z** and **UL766** (0.1 mM each) in PBS buffer, pH 7.4. A 1.5 mL vial containing the solution was irradiated at a distance of 3 cm by a 150 W Xenon lamp with a 620 nm long-pass filter.

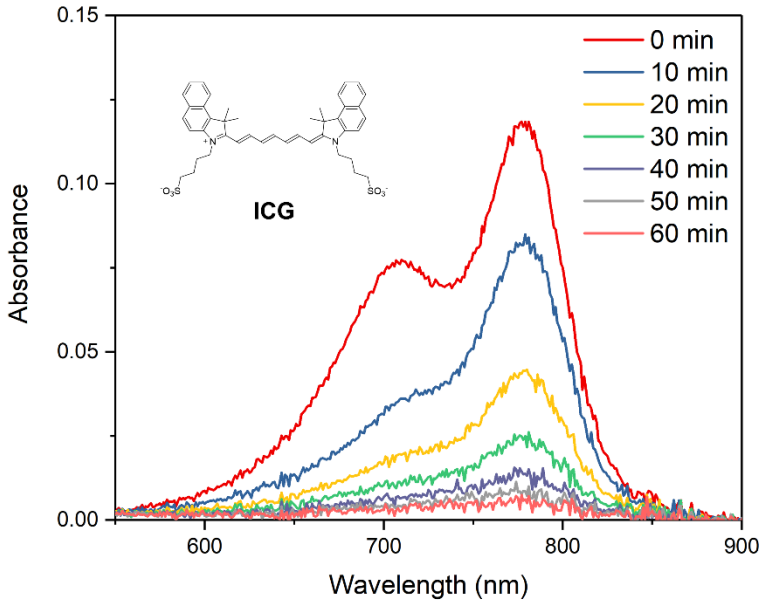

Figure S15. Absorption change of **ICG** (1 μM, PBS, 23 °C) irradiated by a Xenon lamp with a 620 nm long-pass filter.

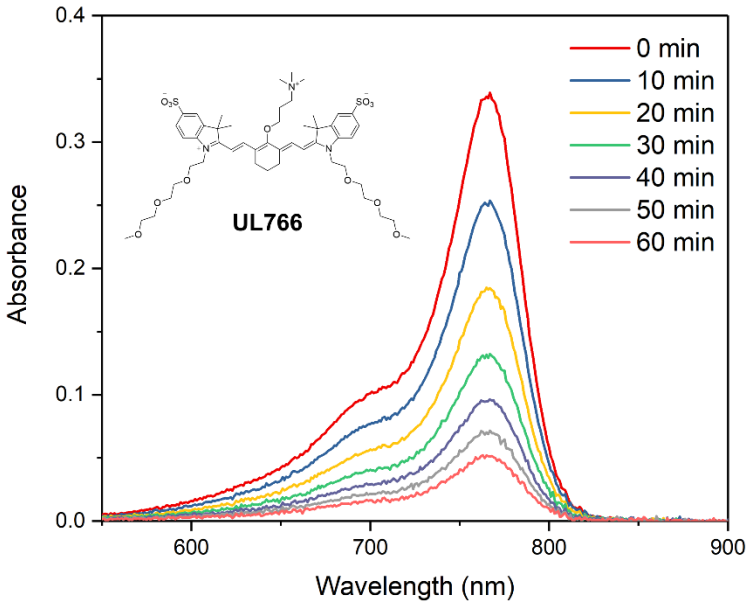

Figure S16. Absorption change of **UL766** (1 μM, PBS, 23 °C) irradiated by a Xenon lamp with a 620 nm long-pass filter.

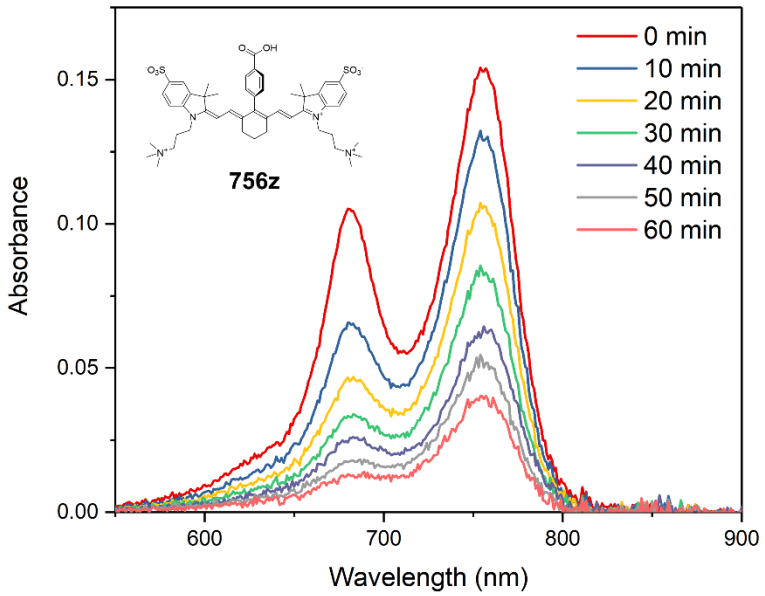

Figure S17. Absorption change of **756z** (1 μM, PBS, 23 °C) irradiated by a Xenon lamp with a 620 nm long-pass filter.

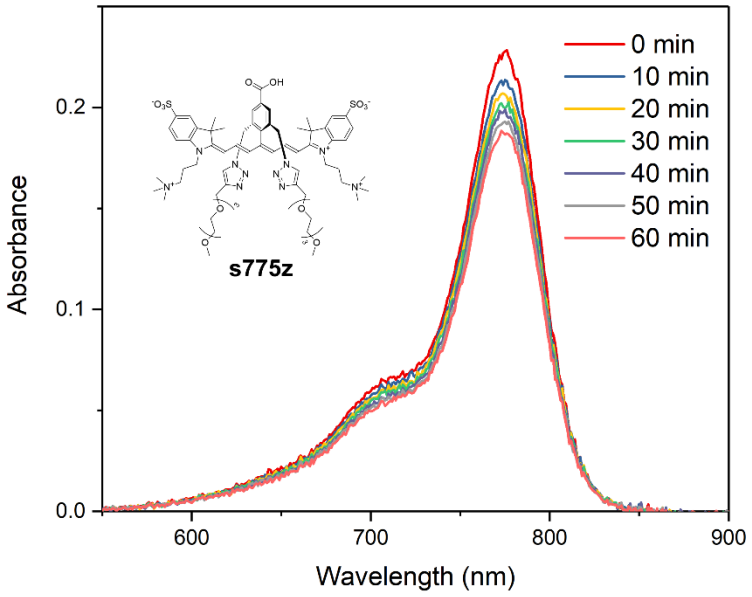

Figure S18. Absorption change of **s775z** (1 μM, PBS, 23 °C) irradiated by a Xenon lamp with a 620 nm long-pass filter.

Table S3. Rate constant and half-life of the first-order decay of heptamethine dyes in pH 7.4 PBS under a 150 W Xenon lamp irradiation at 23 °C.

Dye	k (s^{-1})	$t_{1/2}$ (s)
ICG	8.7×10^{-4}	8.0×10^{2}
UL766	5.3×10^{-4}	1.3×10^{3}
756z	3.7×10^{-4}	1.9×10^{3}
s775z	5.0×10^{-5}	1.4×10^{4}

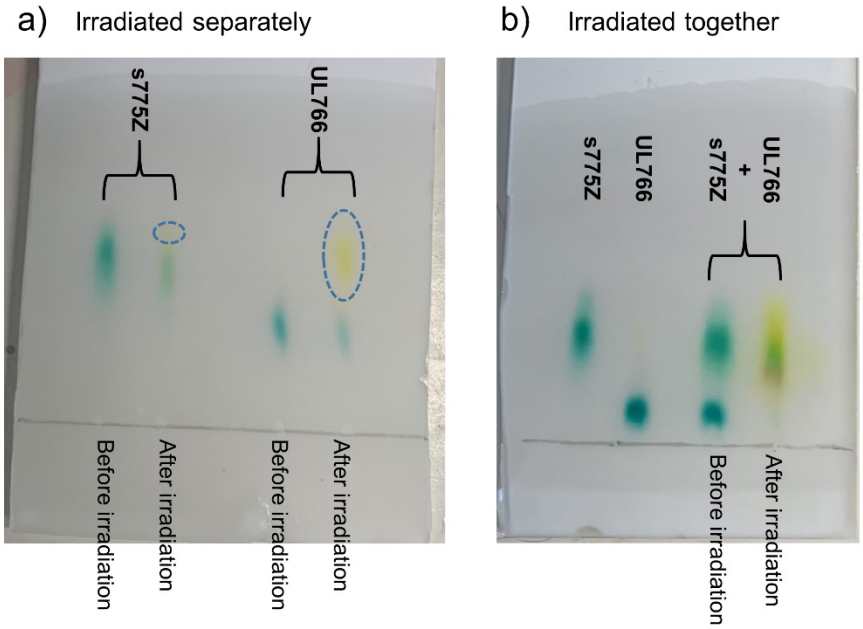

Figure S19. TLC analysis (C18, eluent: MeOH/H_2O = 1/1, v/v + 1% TFA) of **s775z** and **UL766** before and after Xenon lamp irradiation for 2 hr. a) separate samples (0.1 mM in H_2O) of **s775z** (Rf = 0.5) and **UL766** (Rf = 0.3) before and after irradiation; notably, the primary photodegradation product of **UL766** is the yellow spot at (Rf = 0.5) on the TLC plate. In the case of **s775z** there is also a very small yellow spot at higher Rf = 0.6 due to small amount of photodegradation. b) A binary mixture of **s775z** and **UL766** (0.1 mM of each dye in H_2O) was irradiated; notably, the **UL766** spot disappeared completely but a moderate amount of the **s775z** spot remained. Thus, the **s775z** is more resistant than **UL766** to photobleaching by the same amount of singlet oxygen in this competitive experiment.

In Vivo Station Irradiation

Imaging phantoms were created by immobilizing 100 µL drops on a non-reflective black surface, and two sets of phantoms (each N=3) composed of **s775z** or **UL766** (10 µM) in PBS buffer, pH 7.4, were located inside an in vivo imaging station (Ami HT Spectral Imaging). An initial fluorescence intensity image of the phantoms was acquired (ex: 745 nm, em: 850 nm, exposure: 5 sec, percent power: 50%, F-stop: 2, binning: small, FOV: 10). Then, the phantoms were simultaneously irradiated inside the imaging station for four intervals of 15 min (ex: 745 nm, em: 850 nm, percent power: 100%, F-stop: 2, binning: small; FOV: 10). After each 15 min interval, a fluorescence intensity image of the phantoms was acquired and the mean pixel intensity (MPI) of each individual phantom was determined using ImageJ2 software.

10. Synthesis and Characterization of s775z-IgG and 756z-IgG

Antibody Conjugation

Goat IgG (Sigma-Aldrich, I5256) was dissolved in 150 mM NaCl to give a 10 mg/mL solution and was further diluted to 1 mg/mL using buffer A (150 mM Na_2CO_3, pH 9.3). A 10 µL aliquot of dye NHS ester (**756z** or **s775z**) in DMSO was added to 200 µL of goat IgG (1 mg/mL) to give a stoichiometry of reactants (antibody: dye NHS ester) of 1:10, 1:15, 1:30, or 1:50 (the final DOL for the samples of **s775z-IgG** was 0.6, 0.9, 1.7, 2.3). The reaction was incubated at room temperature with mixing by light vortex every 10 min. After 30 min, the reaction was filtered using a PD-10 desalting column (GE Healthcare Life Sciences) pre-equilibrated with buffer B (575 mM NaCl, 37.5mM NaH_2PO_4, 0.75 mM EDTA, pH 7.5). The eluent was collected and concentrated using an Amicon® ultra-4 centrifugal filter unit. Each antibody conjugate was washed several times with buffer B and concentrated. To get DOL of 4.3 or 10.7 for samples of **s775z-IgG** the labeling reaction used a stoichiometry of reactants (antibody: **s775z** NHS ester) of 1:100 or 1:500. These reactions were incubated at room temperature with mixing by light vortex every 15 min. After 60 min, the **s775z-IgG** conjugates were filtered twice using the PD-10 desalting column and concentrated using the same procedure as described above.

Proof of Purity by Polyacrylamide Gel Electrophoresis

Aqueous samples of purified **s775z-IgG** or **756z-IgG** were loaded into a 4-15% Mini-PROTEAN TGX precast protein gel (Bio-Rad). The gel was run at 125 V for 45 min and was then imaged with an *in vivo* imaging station (Ami HT Spectral Instruments Imaging) (ex: 745 nm, em: 850 nm, exposure: 3 sec, percent power: 50%, F-stop: 2, binning: small). Next, the gel was stained overnight with Coomassie blue and photographed in ambient light. The calculated fluorescence mean pixel intensity of each band was divided by the calculated Coomassie blue mean pixel intensity, using ImageJ2 software to give the corrected fluorescence. Figure 5b shows a plot of DOL for **756z-IgG** or **s775z-IgG** versus corrected fluorescence intensity (corrected for protein concentration and normalized relative to the value for **s775z-IgG** DOL 10.7).

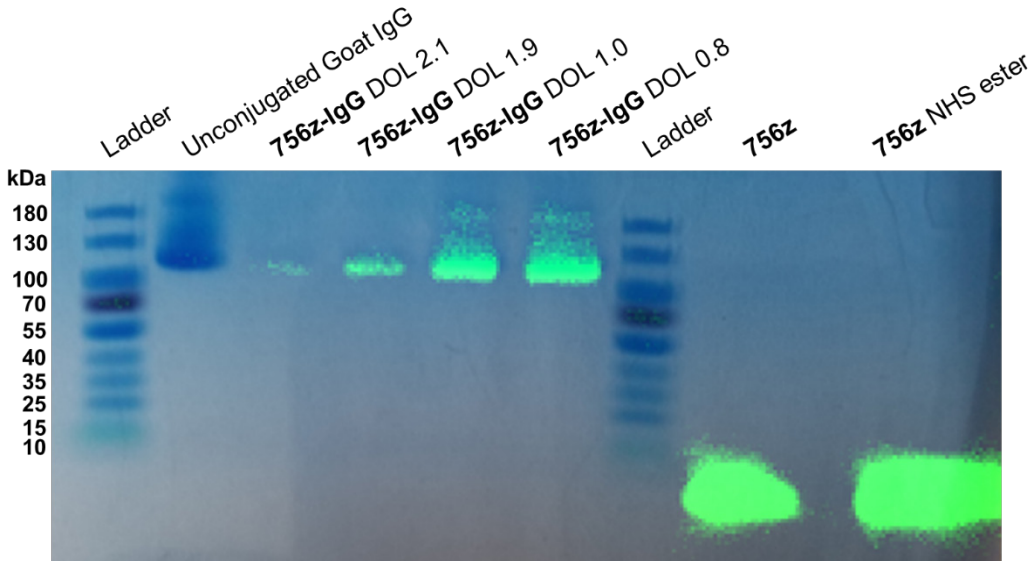

Figure S20. Polyacrylamide gel (4-15%) loaded with protein ladder, unconjugated goat IgG, **756z -IgG**, **756z**, and **756z** NHS ester. Gel was photographed in ambient light following a Coomassie blue stain and overlaid with a fluorescent image acquired with an in vivo imaging station (Ami HT Spectral Instruments Imaging) (ex: 745 nm, em: 850 nm, exposure: 3 sec, percent power: 50%, F-stop: 2, binning: small). DOL; degree of labeling.

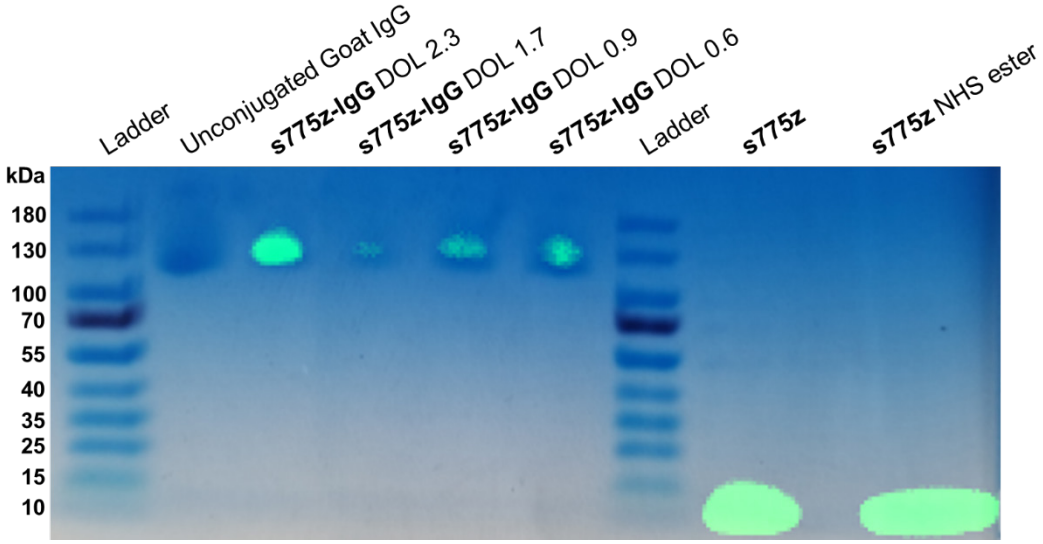

Figure S21. Polyacrylamide gel (4-15%) loaded with protein ladder, unconjugated goat IgG, **s775z-IgG**, **s775z**, and **s775z** NHS ester dye. Gel was photographed in ambient light following a Coomassie blue stain and overlaid with a fluorescent image acquired with an in vivo imaging station (Ami HT Spectral Instruments Imaging) (ex: 745 nm, em: 850 nm, exposure: 3 sec, percent power: 50%, F-stop: 2, binning: small). DOL; degree of labeling.

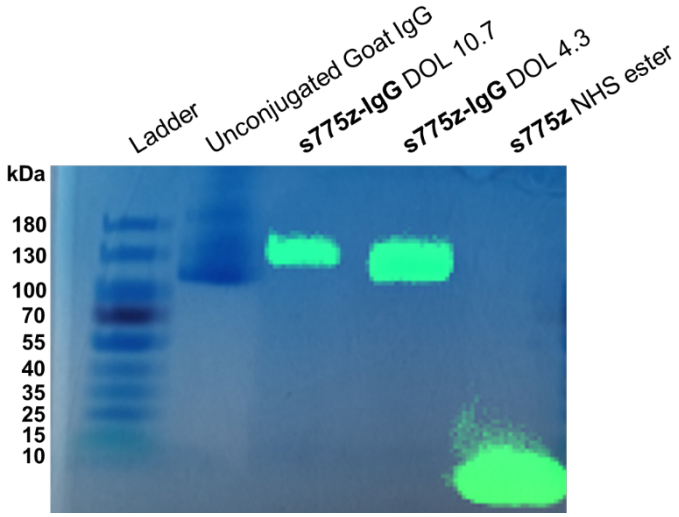

Figure S22. Polyacrylamide gel (4-15%) loaded with protein ladder, unconjugated goat IgG, **s775z-IgG**, and **s775z** NHS ester. Gel was photographed in ambient light following a Coomassie blue stain and overlaid with a fluorescent image acquired with an in vivo imaging station (Ami HT Spectral Instruments Imaging) (ex: 745 nm, em: 850 nm, exposure: 3 sec, percent power: 50%, F-stop: 2, binning: small). DOL; degree of labeling.

Antibody Conjugate Absorbance

Absorbance spectra of goat IgG antibody bioconjugates were collected in buffer B (575 mM NaCl, 37.5 mM NaH_2PO_4 and 0.75 mM EDTA in water, pH 7.5) using Implen NanoPhotometer NP80. Spectra were normalized to absorbance at 280 nm. The degree of labeling (DOL) was calculated using the maximum method with the following equation where A_{max} is the maximum absorbance due to monomer heptamethine dye, A_{280} is the absorbance at 280 nm, $\epsilon_{antibody}$ is 210,000 $M^{-1}cm^{-1}$, C_{280} is 0.11 and takes into account the absorbance contribution from covalently bound heptamethine dye at 280 nm, [10] ϵ_{max} is 111,000 $M^{-1}cm^{-1}$ for the monomer peak of **756z**, and ϵ_{max} is 204,000 $M^{-1}cm^{-1}$ for the monomer peak of **s775z**:

$$DOL = \frac{A_{max}\epsilon_{antibody}}{(A_{280}-A_{max}C_{280})\epsilon_{max}}$$

The same values of DOL were obtained when the alternative peak integration method was used to analyze the data. [11]

Antibody Conjugate Fluorescence

Fluorescence emission spectra of dye labelled goat IgG were collected in buffer B (575 mM NaCl, 37.5 mM NaH_2PO_4 and 0.75 mM EDTA in water, pH 7.5) using Horiba Fluoromax-4 Fluorometer with FluorEssence software (ex: 745 nm, slit width: 4 nm). The fluorescence emission spectra were divided by the fluorescence emission intensity at 355 nm (ex: 280 nm, slit width: 2 nm) to obtain corrected spectra that accounts for variations in antibody concentration.

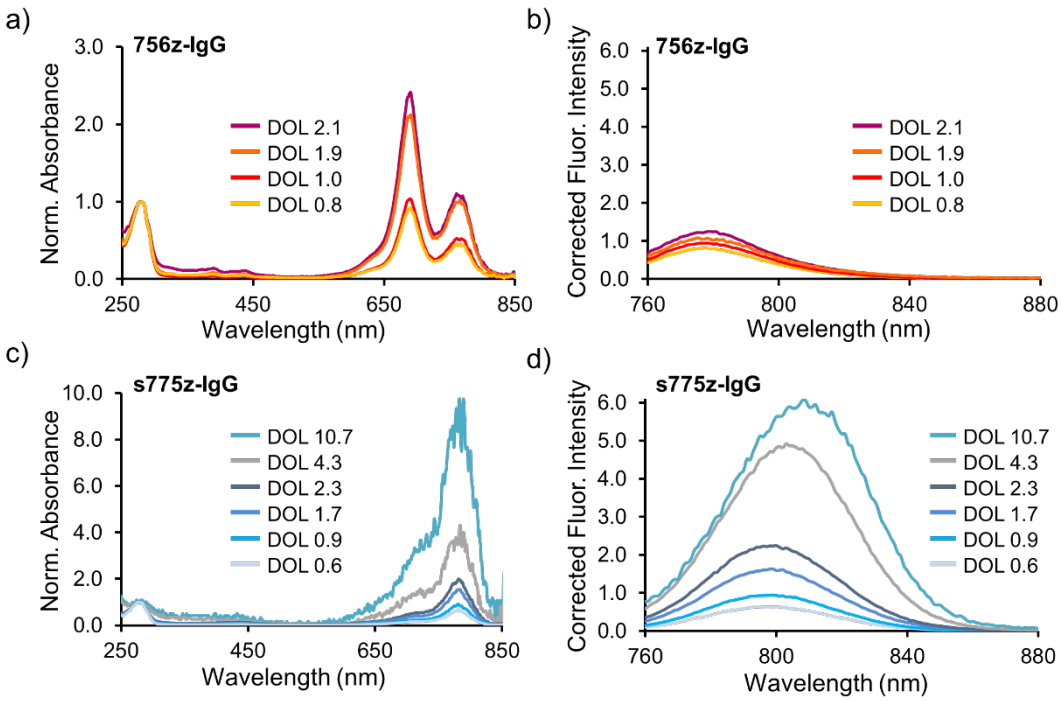

Figure S23. Photophysical properties of goat IgG antibody bioconjugates. Absorbance and emission spectra in buffer B for a), b) **756z-IgG** and c), d) **s775z-IgG**. Absorbance spectra were normalized to the absorbance at 280 nm. Emission spectra (ex: 745 nm, slit width 4 nm) were divided by the fluorescence emission intensity at 355 nm (ex: 280 nm, slit width: 2 nm) to obtain corrected fluorescence spectra that accounts for variations in antibody concentration. DOL, degree of labeling.

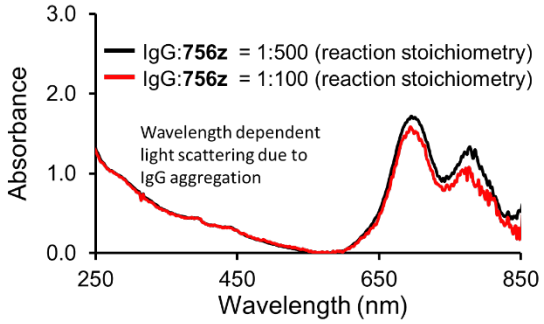

Figure S24. Absorbance spectra for pure samples of **756z-IgG** with DOL > 2.1 that were obtained by reacting IgG with a large excess of reactive NHS ester of **756z**. The wavelength dependent scattering of illumination light (scattering increases with shorter wavelength) is caused by aggregates of **756z-IgG**. Solvent is buffer B.

SUPPORTING INFORMATION

Storage Stability of Antibody Conjugates

Absorbance spectra of **756z-IgG (**DOL 2.1) and s**775z-IgG (**DOL 2.3) were collected in buffer B using Implen NanoPhotometer NP80. Spectra were acquired at 0, 2, 4, and 7 days after bioconjugation and were normalized to the absorbance at 280 nm. The antibody conjugates were stored at 4℃ between data collection.

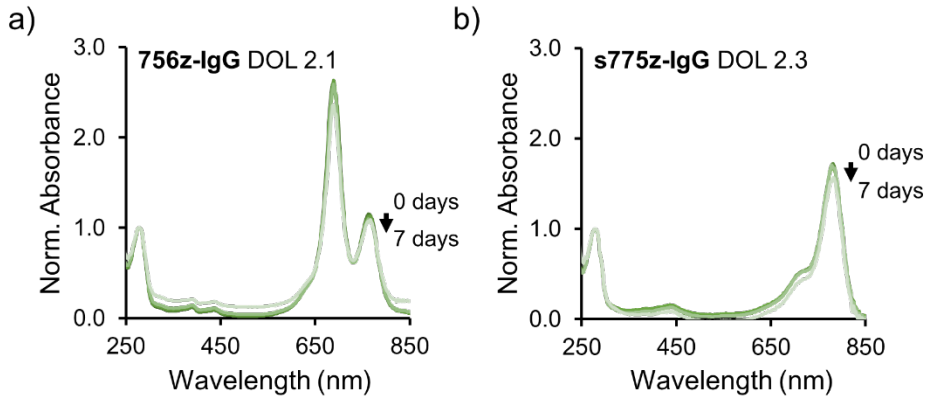

Figure S25. Stability of antibody conjugates at 4 ºC in buffer B over 7 days. Absorbance spectra of a) **756z-IgG** DOL 2.1 and b) **s775z-IgG** DOL 2.3.

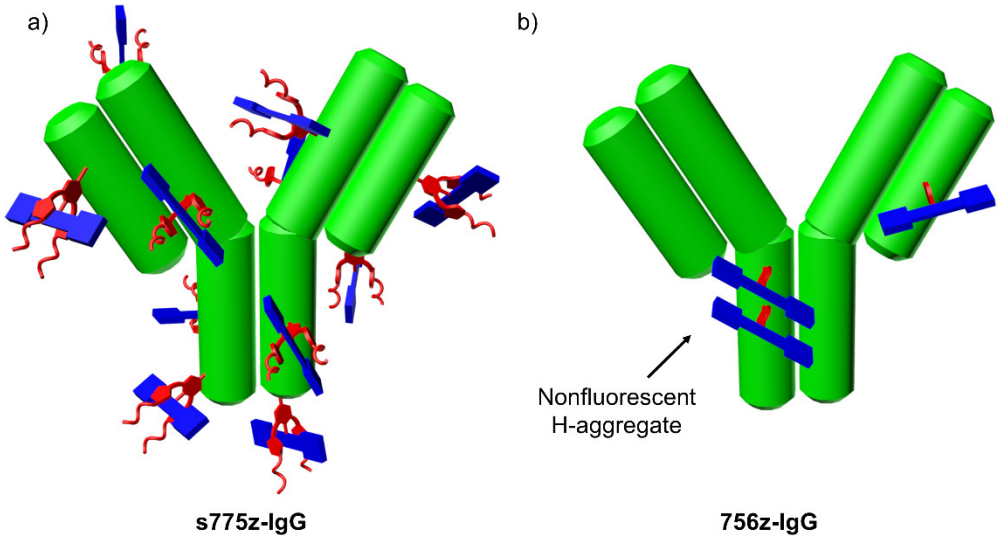

Scheme S1. Schematic picture of IgG antibody labeled with: a) eleven copies of **s775z** to give **s775z-IgG** DOL = 11, the two red shielding arms on each blue fluorochrome ensures that the **s775z** NHS ester molecules react with lysine residues that are quite separated from each other on the antibody surface. b) three copies of **756z** to give **756z-IgG** DOL = 3, the propensity of **756z** NHS ester molecules to self-aggregate favors dye attachment at proximal lysine positions on the IgG surface (stacked appended fluorochromes) leading to a highly quenched (non-fluorescent) antibody-dye conjugate that exhibits a strong “H-aggregate” peak at 680 nm in the absorption spectrum.

11. Cell Experiments

Cell viability

CHO-K1 cells (Chinese hamster ovary, ATCC® CCL-61™) and A549 cells (human lung adenocarcinoma, ATCC® CCL-185™) were cultured and maintained in F-12K medium (supplemented with 10% fetal bovine serum, 1% penicillin streptomycin) at 37 °C and 5% CO_2 in a humidified incubator. For cell viability studies, CHO-K1 or A549 cells were seeded into 96-microwell plates and grown to 70% confluency. The medium was then removed and replaced with either **s775z** or **ICG** at various concentrations (N = 3) in F12-K medium for 24 hr at 37 °C and 5% CO_2 in a humidified incubator. After 24 hr, the dye was removed and replaced with F-12K medium containing [3-(4,5-dimethylthiazol-2-yl)-2,5-diphenyltetrazolium bromide] (MTT, 1.1 mM). The samples were incubated at 37 °C and 5% CO_2 for 2 hr and an SDS−HCl detergent solution was then added. The samples were incubated overnight, and the absorbance of each well was measured at 570 nm, where the readings were normalized relative to untreated cells. All measurements were done in triplicate.

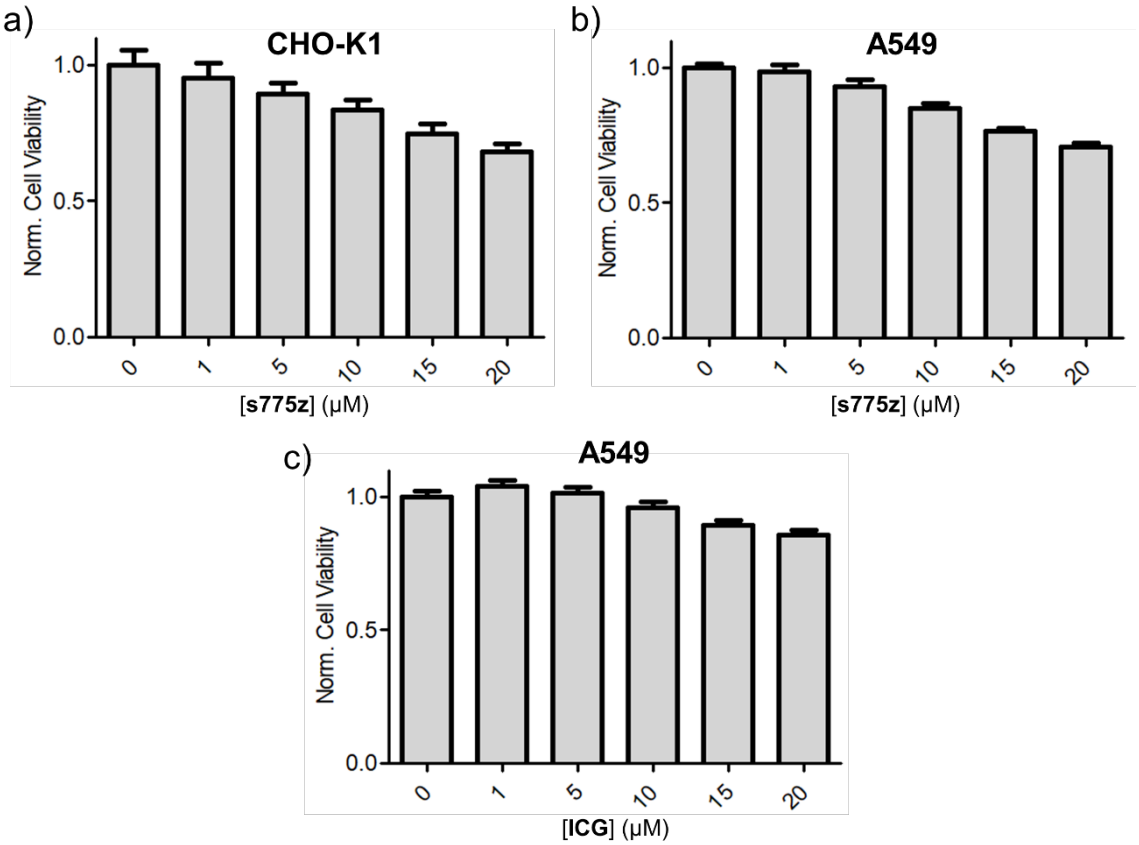

Figure S26. MTT cell viability assay. a) CHO-K1 cells were treated for 24 hr at 37 °C, 5% CO_2 with **s775z**. A549 cells were treated for 24 hr at 37 °C, 5% CO_2 with either b) **s775z** or c) **ICG**.

SUPPORTING INFORMATION

Cell Microscopy

For fluorescence microscopy, A549 cells were seeded and grown to 70% confluency on an 8-well chambered coverglass (Lab-Tek, Nunc, USA). The media was removed, and the cells were separately incubated with 10 μM dye (**756z**, **756z-RGD**, **s775z**, or **s775z-RGD**) in media for 1 hr at 37 °C. For blocking, 100 μM of cRGDfK was added to the cells, 10 min prior to dye treatment and remained present during NIR dye incubation. After dye incubation, the cells were washed several times with PBS, fixed with 4% cold paraformaldehyde for 20 min at room temperature and washed again with PBS. The cells were then co-stained with 3 μM Hoechst 33342 for 10 min, washed with PBS, and imaged on a Zeiss Axiovert 100 TV epifluorescence microscope equipped with a custom filter (ex: 445/40, em: 494/20) and ICG filter (ex: 769/41, em: 832/37). For each micrograph, a background subtraction with a rolling ball radius of 20 pixels was applied using ImageJ2 software. Next, a triangle threshold was employed and used to calculate the average mean pixel intensity (MPI) where overall averages and SEM were calculated and plotted in GraphPad Prism. A total of 6 micrographs were evaluated per condition and each experiment was conducted in triplicate.

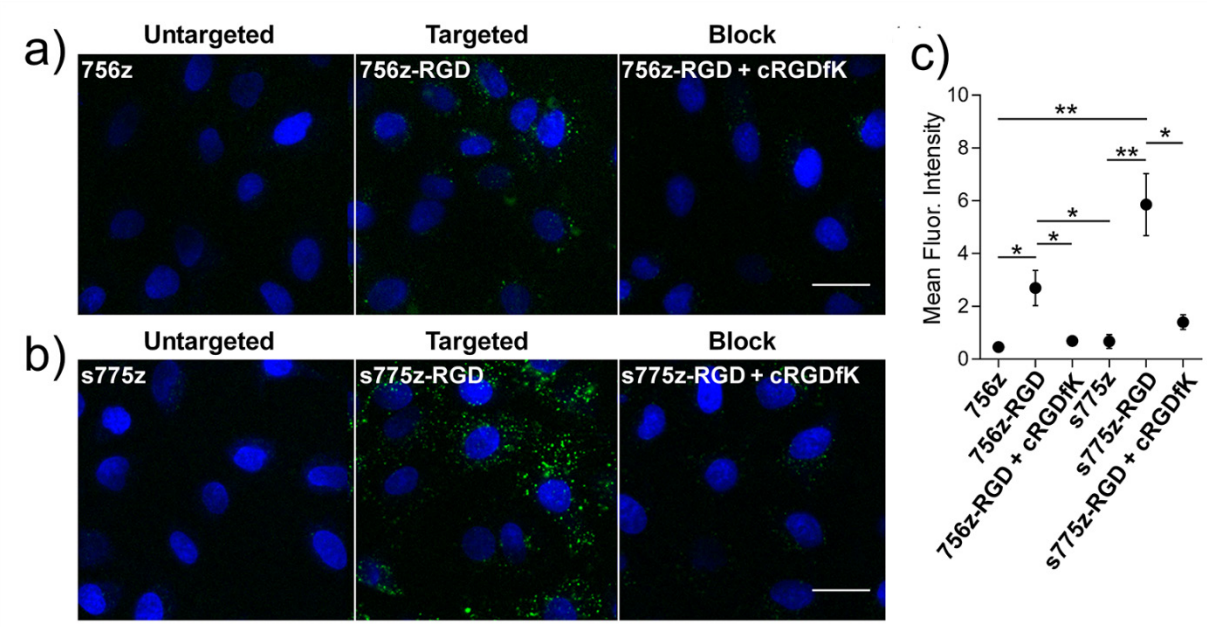

Figure S27. Representative epifluorescence micrographs of integrin positive A549 cells that were treated for 1 hr with 10 μM of either (a) unshielded **756z** or its targeted analogue **756z-RGD,** (b) shielded **s775z** and its targeted analogue **s775z-RGD**. The two targeted dyes contain a cyclic peptide cRGDfK sequence for targeting the overexpressed cell surface integrin receptors. The blocking experiments added 100 μM of free cRGDfK prior to the incubation with RGD probes. NIR heptamethine fluorescence is shown in green, and Hoechst nuclear stain is shown in blue. Scale bar = 30 μm. (c) Quantification of intracellular mean fluorescence intensities as a measure of NIR dye internalization (6 micrographs per condition and 3 replicates). * indicates $p < 0.05$, and ** $p < 0.01$.

SUPPORTING INFORMATION

12. Mouse Biodistribution

All animal experiments were conducted under protocols that were approved by the Notre Dame Institutional Animal Care and Use Committee. Female SKH1 hairless mice (N = 4) were divided into two cohorts and received a retro-orbital injection of **ICG** or **s775z** (50 µL, 10 nmol). Five min prior to injection, each mouse was anesthetized with 2-3% isoflurane with an oxygen flow rate of 2 L min^{-1} and imaged using an in vivo imaging station (Ami HT Spectral Imaging) (ex: 745 nm, em: 850 nm, exposure: 3 sec, percent power: 50%, F-stop: 2, binning: small, FOV: 20). The mice were then injected with dye and imaged at 0, 1, and 2 hr. At 2 hr, the mice were anesthetized, sacrificed via cervical dislocation, and blood was collected from the heart. The lower cavity of the mice was then exposed and imaged. Next, all major organs were removed and imaged including the liver (without gallbladder), heart, lungs, spleen, kidneys, skin, muscle, and intestines. The images were pseudocolored "fire," and an arbitrary maximum fluorescence value was chosen. Biodistribution analysis was performed by importing images of the excised organs from each mouse into ImageJ2. The amount of dye was then quantified by manually drawing a region of interest around each organ. The MPI of each organ was measured and divided by the MPI for thigh muscle from the same animal.

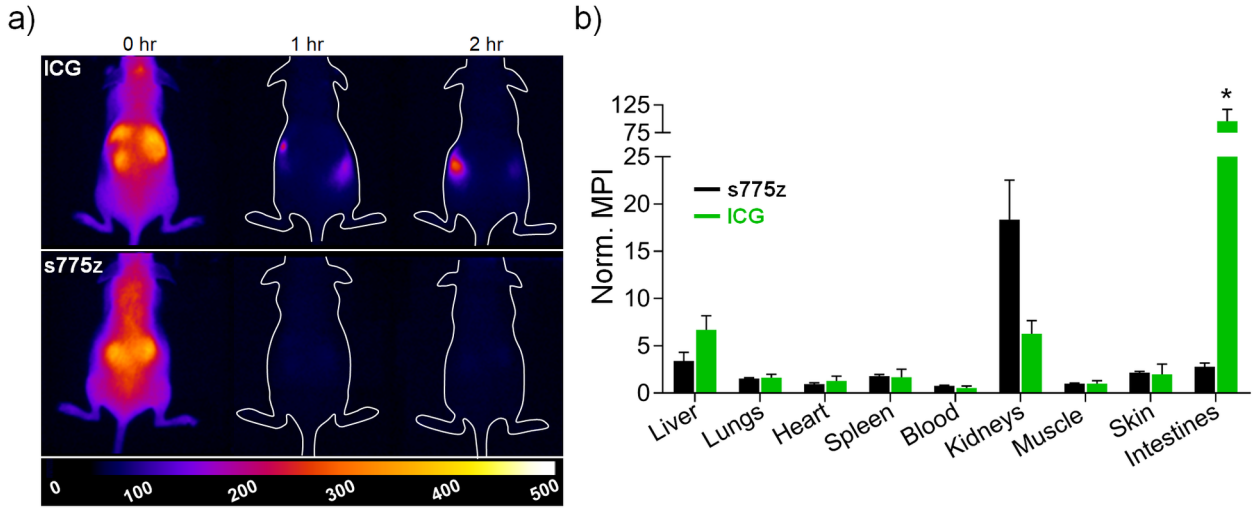

Figure S28. a) Representative whole-body NIR fluorescence images of living SKH1 hairless mice at 0, 1, and 2 hr after intravenous injection of either **ICG** or **s775z** (10 nmol). b) In vivo biodistribution of **s775z** and **ICG** in normal mice. The SKH1 hairless mice (N = 4) received an intravenous injection of **ICG** or **s775z** (10 nmol) and were sacrificed after 2 hr. The mean pixel intensity (MPI) for each excised organ is relative to the MPI for thigh muscle from the same animal; error bars indicate ±SEM. * indicates $p < 0.05$. Note: the y-axis is truncated.

SUPPORTING INFORMATION

13. Mouse Tumor Imaging

All animal experiments were conducted under protocols that were approved by the Notre Dame Institutional Animal Care and Use Committee. Female Foxn1 nude mice (N = 8) were inoculated with A549 cells (1 x 10^6) in Corning Matrigel matrix on the right rear flank. Approximately 4 weeks later, the mice were divided into two cohorts and received a retro-orbital injection of either **s775z** or **s775z-RGD** (10 nmol in 50 µL saline). Five min prior to injection, each mouse was anesthetized with 2-3% isoflurane with an oxygen flow rate of 2 L min^{-1} and imaged using an in vivo imaging station (Ami HT Spectral Imaging) (ex: 745 nm, em: 850 nm, exposure: 3 sec, percent power: 50%, F-stop: 2, binning: small, FOV: 20). The mice were then injected with dye and imaged at 0, 0.5, 1, 2, and 3 hr. At 3 hr, the mice were anesthetized and sacrificed via cervical dislocation, and blood was collected from the heart. To simulate a surgery, the mice were imaged prior to surgery, the fluorescent tumor was fully removed, and the mice were imaged again. Next, all major organs were removed and imaged including the liver, heart, lungs, spleen, kidneys, skin, and muscle. For image processing, the whole body and tumor images were pseudocolored "fire," and an arbitrary maximum fluorescence value was chosen. Biodistribution analysis was performed by importing NIR fluorescence images of the excised organs from each mouse into ImageJ2 and the amount of dye in each organ was quantified by manually drawing a region of interest around each organ and determining the fluorescence MPI. The value was divided by the MPI for the thigh muscle from the same animal to give a normalized MPI.

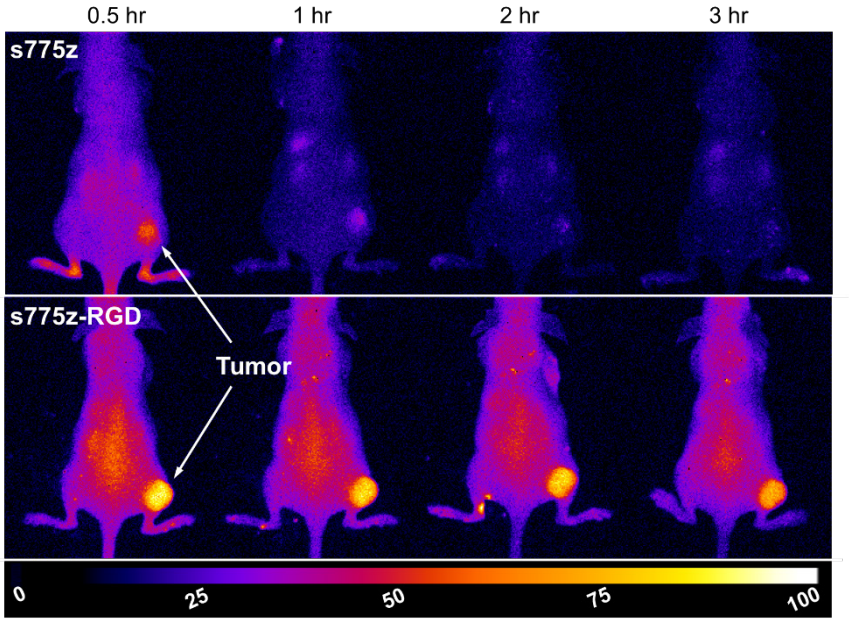

Figure S29. Representative whole-body fluorescence images of living nude mice bearing a subcutaneous tumor *(human A549 cells)* at 0.5, 1, 2, and 3 hr after intravenous injection of either **s775z** or **s775z-RGD** (10 nmol). Fluorescence intensity scale in arbitary units.

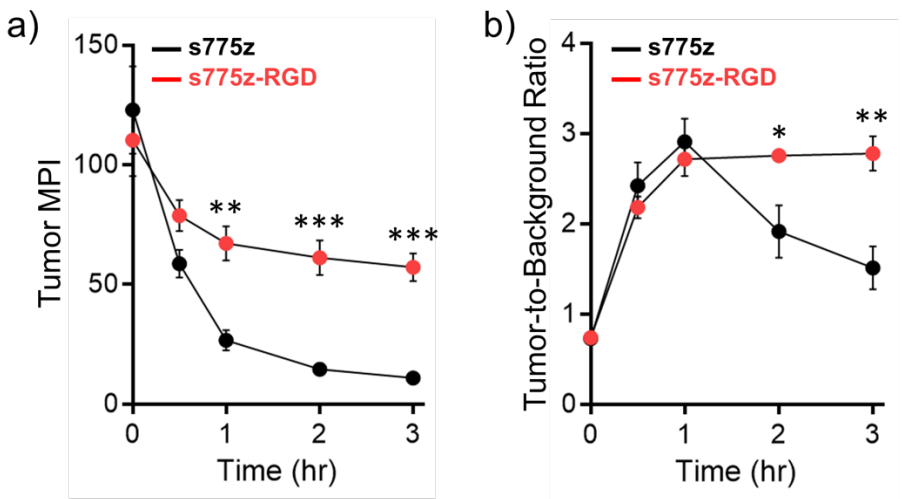

Figure S30. a) Tumor MPI, and b) Tumor-to-Background Ratio for living nude mice bearing a subcutaneous tumor *(human A549 cells)* after intravenous injection of **s775z** or **s775z-RGD** (10 nmol). The fluorescence mean pixel intensity (MPI) of two regions of interest (equal sizes) on the fluorescent images (tumor or background site on the opposite flank), at different post-injection time points, were measured using ImageJ2 software and used to calculate values for Tumor MPI, and Tumor-to-Background Ratio. * indicates $p<0.05$, ** $p<0.01$, and *** $p<0.001$.

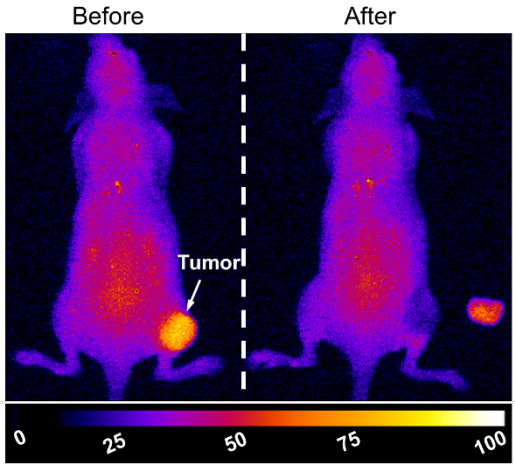

Figure S31. Representative NIR fluorescence images of a nude mouse bearing a subcutaneous tumor *(human A549 cells)* at 3 hr after intravenous injection of **s775z-RGD** (10 nmol). Images were taken before mock surgery and after the tumor was fully excised. Fluorescence intensity scale in arbitary units.

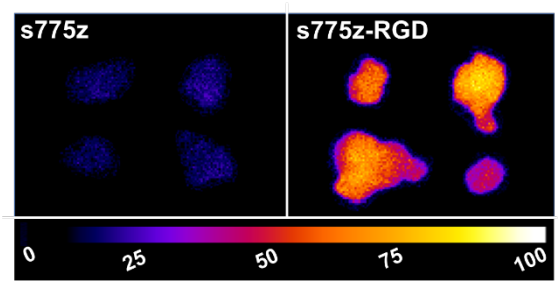

Figure S32. NIR fluorescence images of excised subcutaneous tumors *(human A549 cells)* that were harvested from different mice at 3 hr after intravenous injection of either **s775z** or **s775z-RGD** (10 nmol) (each N = 4). Fluorescence intensity scale in arbitary units.

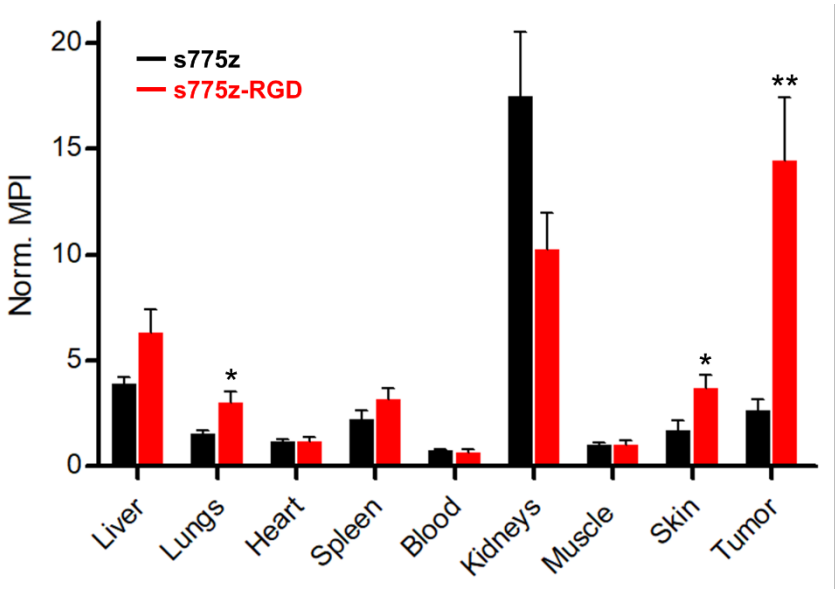

Figure S33. Biodistribution of **s775z** and **s775z-RGD** in tumor-bearing mice. A549 xenograft nude mice received an intravenous injection of either **s775z** or **s775z-RGD** (10 nmol) and were sacrificed after 3 hr. The mean pixel intensity (MPI) for each excised organ is relative to the MPI for thigh muscle from the same animal; error bars indicate ±SEM. * indicates p<0.05, and ** p<0.01.

Statistical Analysis

For cell microscopy and in vivo imaging, an unpaired t test using GraphPad Prism software was applied. Statistical significance between experimental conditions was defined as a p-value less than 0.05, and p-values were assigned in the following manner: * $p < 0.05$, ** $p < 0.01$, *** $p < 0.001$.

14. Molecular Modeling

Molecular modeling employed the semiempirical method within the MOPAC program.[12] The dielectric constant of the solvent was set at 78.4 for water and 25 °C. The model of **s775z** in manuscript Scheme 2 was generated at the AM1 level. Structures of **s775z** generated using the more modern PM7 level exhibited distorted chain conformations due to an internal ion-pairing artifact. The structure shown in Figure S34 does not show this artifact because the two terminal cationic trimethylammonium groups were treated as neutral hydrocarbon isosteres. Most importantly, both the AM1 and PM7 models show the same key structural features; that is, the polyene adopts an all-trans conformation and the plane of the meso-Aryl ring is strongly twisted out of the plane of the heptamethine polyene.

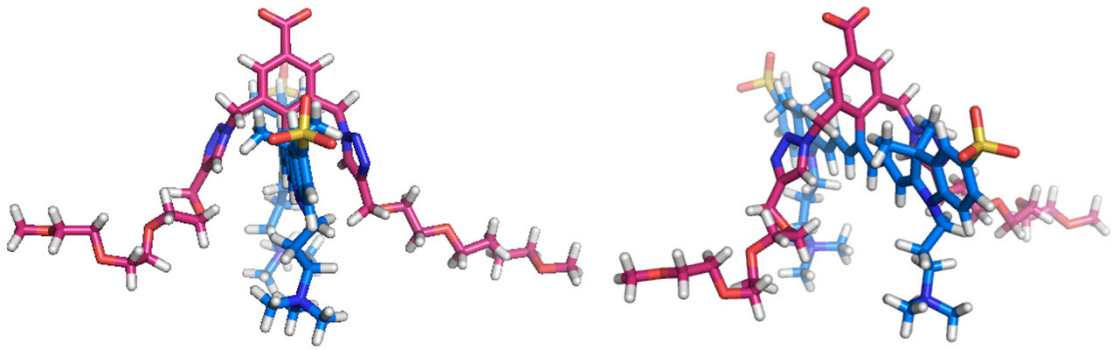

Figure S34. Molecular model of a close analogue of **s775z** (both terminal cationic trimethylammonium groups treated as neutral hydrocarbon isosteres) at the PM7 level performed by the MOPAC program. Two views of the same model.

Cartesian Coordinates of **s775z** at the AM1 Level

TOTAL ENERGY = -17606.22651 EV

FINAL GEOMETRY OBTAINED
EPS=78.4 AM1 CHARGE=0 EF xyz GNORM=0.100 SHIFT=80

C	-1.80913143 +1	0.93187046 +1	0.49725729 +1
C	-0.68752470 +1	1.69847792 +1	0.31434270 +1
C	-0.76283231 +1	3.16688017 +1	0.39283311 +1
C	-0.94498092 +1	3.91442813 +1	-0.79145339 +1
C	-1.21815581 +1	5.28322909 +1	-0.72308292 +1
C	-1.25945207 +1	5.93934394 +1	0.50938675 +1
C	-0.98859902 +1	5.22090845 +1	1.66942185 +1
C	-0.74733617 +1	3.83641124 +1	1.62721072 +1
C	0.55491902 +1	1.01735567 +1	0.03587546 +1
C	1.77287954 +1	1.56669700 +1	-0.18601928 +1
C	2.91810634 +1	0.71411365 +1	-0.36933309 +1
C	4.20409924 +1	1.09873124 +1	-0.57037381 +1
N	5.28124272 +1	0.17387142 +1	-0.71111801 +1
C	4.73964420 +1	2.53500899 +1	-0.76614698 +1
C	6.21817348 +1	2.29735742 +1	-0.99292406 +1
C	6.48067849 +1	0.89623401 +1	-0.89503796 +1
C	5.30648976 +1	-1.11122477 +1	-0.05157183 +1
C	7.78512587 +1	0.41177792 +1	-1.01467902 +1
C	7.24399904 +1	3.18332169 +1	-1.24111711 +1
C	8.55821631 +1	2.70453575 +1	-1.38774813 +1
C	8.80266839 +1	1.33496319 +1	-1.26266545 +1
C	-3.11745083 +1	1.42923951 +1	0.77951804 +1
C	-4.18727562 +1	0.58251321 +1	0.87948437 +1
C	-5.50964838 +1	0.96254153 +1	1.23270432 +1
N	-6.56544726 +1	0.10560574 +1	1.26910547 +1
C	-5.96088571 +1	2.37628589 +1	1.69988822 +1
C	-7.42080738 +1	2.13898285 +1	2.02639670 +1
C	-7.72867316 +1	0.77151159 +1	1.76993435 +1
C	-6.64433727 +1	-1.25925383 +1	0.78598494 +1
C	-5.83436170 +1	3.38493670 +1	0.57290246 +1
C	-5.20160272 +1	2.80883927 +1	2.93891131 +1
C	-8.40192289 +1	2.99177059 +1	2.49266574 +1
C	-9.69580059 +1	2.49379211 +1	2.71834455 +1
C	-9.96826182 +1	1.14433471 +1	2.49643000 +1
C	-8.99559298 +1	0.25611426 +1	2.02267981 +1

C	-1.60572412 +1	7.39430072 +1	0.58376636 +1
O	-1.78819808 +1	8.06078551 +1	-0.48256839 +1
O	-1.72900775 +1	7.96225324 +1	1.71379750 +1
C	-0.78058529 +1	3.33819004 +1	-2.17053842 +1
N	-1.55861434 +1	2.15187190 +1	-2.47701135 +1
N	-2.89756611 +1	2.02046188 +1	-2.34428380 +1
N	-3.25385481 +1	0.83518533 +1	-2.64764621 +1
C	-2.12216118 +1	0.07500657 +1	-3.01534821 +1
C	-1.00994738 +1	0.93915837 +1	-2.91276638 +1
C	-2.06299969 +1	-1.36627500 +1	-3.35037943 +1
O	-3.33509668 +1	-1.99637251 +1	-3.40507298 +1
C	-3.86893696 +1	-2.15211374 +1	-4.71270718 +1
C	-0.56373748 +1	3.23183874 +1	2.99374477 +1
N	0.05915979 +1	1.93010318 +1	3.10740378 +1
C	-0.63242868 +1	0.75209082 +1	3.42142301 +1
C	0.38235573 +1	-0.21512881 +1	3.56577817 +1
N	1.60768418 +1	0.45176618 +1	3.33814580 +1
N	1.38924295 +1	1.67858996 +1	3.08061296 +1
C	0.18806557 +1	-1.63215140 +1	3.93238718 +1
O	1.10866355 +1	-2.44898593 +1	3.20567687 +1
C	0.83149734 +1	-3.83852154 +1	3.34534680 +1
H	-1.71349926 +1	-0.16879797 +1	0.41246918 +1
H	-1.40731539 +1	5.86538956 +1	-1.64210763 +1
H	-0.98710195 +1	5.75259851 +1	2.63787674 +1
H	0.47033173 +1	-0.08900998 +1	0.02972793 +1
H	1.91003579 +1	2.66110327 +1	-0.20513621 +1
H	2.68777480 +1	-0.36866206 +1	-0.30575747 +1
H	4.31441230 +1	-1.29062885 +1	0.45308565 +1
H	6.10339982 +1	-1.10417127 +1	0.75062670 +1
C	5.59247111 +1	-2.28331625 +1	-1.00223654 +1
H	8.01533872 +1	-0.65913200 +1	-0.91597874 +1
H	7.04269687 +1	4.26625116 +1	-1.31816285 +1
H	9.83925822 +1	0.96312394 +1	-1.35812273 +1
H	-3.22698214 +1	2.52243173 +1	0.91082100 +1
H	-4.00443002 +1	-0.49435706 +1	0.68474855 +1
H	-5.60304401 +1	-1.65850752 +1	0.61909203 +1
C	-7.45015137 +1	-1.38030899 +1	-0.51268302 +1
H	-7.11886839 +1	-1.87665813 +1	1.60428305 +1
H	-6.29405918 +1	2.99395314 +1	-0.36671327 +1
H	-4.76679933 +1	3.63911273 +1	0.37379626 +1
H	-6.36915533 +1	4.32289198 +1	0.86792194 +1
H	-5.25593308 +1	2.02539826 +1	3.73281501 +1
H	-5.65765400 +1	3.75108274 +1	3.33340054 +1
H	-4.12948319 +1	3.00801045 +1	2.70117660 +1
H	-8.17316538 +1	4.05377034 +1	2.68984336 +1
H	-10.98323399 +1	0.75361670 +1	2.70023568 +1
H	-9.23331367 +1	-0.80738997 +1	1.88088249 +1
H	0.30831995 +1	3.06445068 +1	-2.30808801 +1
H	-1.04526499 +1	4.12590335 +1	-2.93860372 +1
H	0.05240245 +1	0.79570501 +1	-3.11294396 +1
H	-1.52626937 +1	-1.90645348 +1	-2.51687971 +1
H	-1.49460519 +1	-1.50381424 +1	-4.31007934 +1
C	-4.35965691 +1	-0.82710402 +1	-5.28208813 +1
H	-4.72526710 +1	-2.86522269 +1	-4.56815780 +1
H	-3.10794706 +1	-2.61334707 +1	-5.39706972 +1
H	0.04562527 +1	3.95803008 +1	3.61548107 +1
H	-1.58798383 +1	3.14529702 +1	3.46830202 +1
H	-1.71594174 +1	0.69664044 +1	3.52380025 +1
H	-0.86652536 +1	-1.94293649 +1	3.69445241 +1
H	0.37187273 +1	-1.77614479 +1	5.03453426 +1
H	-0.21690344 +1	-4.05887887 +1	3.01230570 +1
C	1.05437932 +1	-4.33449549 +1	4.76865328 +1
H	1.57175141 +1	-4.32731894 +1	2.65558661 +1
C	4.11040719 +1	3.19285156 +1	-1.97930606 +1
H	4.24958478 +1	2.55912027 +1	-2.88771410 +1
H	4.59530843 +1	4.18400541 +1	-2.15586600 +1
H	3.01714810 +1	3.35307603 +1	-1.82009931 +1
C	4.53981786 +1	3.37464836 +1	0.48273701 +1
H	4.94613984 +1	2.84716853 +1	1.37889124 +1
H	3.45826884 +1	3.58679518 +1	0.65378346 +1
H	5.07882778 +1	4.34656629 +1	0.36394004 +1

S	-10.94179308 +1	3.55646368 +1	3.25197724 +1
O	-12.02949886 +1	2.75291867 +1	3.68708228 +1
O	-10.39777059 +1	4.33587856 +1	4.30865752 +1
O	-11.29267893 +1	4.36093791 +1	2.13234698 +1
S	9.84385441 +1	3.76385861 +1	-1.72261727 +1
O	9.42904478 +1	5.08838766 +1	-1.39615697 +1
O	10.14138105 +1	3.64451119 +1	-3.11412643 +1
O	10.95727216 +1	3.35619283 +1	-0.92764416 +1
H	-5.24396647 +1	-0.44712780 +1	-4.70409554 +1
O	-4.84874237 +1	-0.99383808 +1	-6.60533499 +1
H	-3.53764862 +1	-0.06364178 +1	-5.25719352 +1
C	-3.82299466 +1	-1.19143137 +1	-7.58000743 +1
H	-3.63755790 +1	-2.29413010 +1	-7.67663879 +1
H	-2.87643705 +1	-0.67044422 +1	-7.28208314 +1
C	-4.34554642 +1	-0.64393094 +1	-8.90197263 +1
H	-5.43144148 +1	-0.89088026 +1	-9.03230006 +1
H	-3.74982246 +1	-1.07551585 +1	-9.74884713 +1
O	-4.15159513 +1	0.77125771 +1	-8.87207517 +1
C	-4.94742739 +1	1.48015995 +1	-9.81146614 +1
H	-6.00908983 +1	1.11910678 +1	-9.78820203 +1
C	-4.36539031 +1	1.36242597 +1	-11.21689376 +1
H	-4.90898695 +1	2.54468578 +1	-9.45452742 +1
H	-4.12175571 +1	0.29418624 +1	-11.45578339 +1
H	-3.43795495 +1	1.98847660 +1	-11.31284193 +1
O	-5.25743105 +1	1.90542690 +1	-12.18160065 +1
C	-6.30776902 +1	1.02383851 +1	-12.55464762 +1
H	-6.86228042 +1	1.57326479 +1	-13.35612831 +1
H	-6.97949016 +1	0.82017133 +1	-11.68543452 +1
H	-5.89274973 +1	0.06427309 +1	-12.95029238 +1
O	-0.13934980 +1	-4.04629568 +1	5.50109399 +1
H	1.92738164 +1	-3.81157515 +1	5.23926905 +1
H	1.22916117 +1	-5.44238484 +1	4.77205160 +1
C	-0.03149138 +1	-4.31447348 +1	6.89279667 +1
C	0.88323979 +1	-3.30292910 +1	7.58121973 +1
H	0.33512028 +1	-5.35994897 +1	7.06167769 +1
H	-1.08590695 +1	-4.21812541 +1	7.27009630 +1
H	1.93480910 +1	-3.69358973 +1	7.64359451 +1
O	0.49834612 +1	-3.11785838 +1	8.93673297 +1
H	0.88045409 +1	-2.32977200 +1	7.02257908 +1
C	-0.50758942 +1	-2.11791083 +1	9.11344223 +1
H	-1.46750104 +1	-2.46442093 +1	8.64826876 +1
H	-0.17708353 +1	-1.15766721 +1	8.63714497 +1
C	-0.69787007 +1	-1.94128319 +1	10.61338777 +1
H	-0.69479066 +1	-2.93188532 +1	11.13934874 +1
H	-1.66531644 +1	-1.40815982 +1	10.81054000 +1
O	0.38931000 +1	-1.14392369 +1	11.08429312 +1
C	0.33909344 +1	-0.93274453 +1	12.48784660 +1
H	0.36766180 +1	-1.90829053 +1	13.03285612 +1
H	1.25267852 +1	-0.32813627 +1	12.71477892 +1
H	-0.58545614 +1	-0.36807551 +1	12.76361387 +1
H	4.83142078 +1	-2.30763557 +1	-1.82508665 +1
C	5.52707383 +1	-3.56201231 +1	-0.17657571 +1
H	6.60319170 +1	-2.16142971 +1	-1.47251212 +1
H	4.46858974 +1	-3.70802547 +1	0.18615797 +1
H	6.20147086 +1	-3.47318269 +1	0.72452139 +1
N	5.92852110 +1	-4.81661981 +1	-0.90392707 +1
C	5.31730967 +1	-4.86410238 +1	-2.26236058 +1
C	5.44923306 +1	-5.99018380 +1	-0.11022398 +1
C	7.41394526 +1	-4.89323687 +1	-1.02610322 +1
H	7.78447910 +1	-4.03320062 +1	-1.64295358 +1
H	7.68852517 +1	-5.86047648 +1	-1.52552211 +1
H	7.87436263 +1	-4.85545433 +1	-0.00340646 +1
H	4.21266101 +1	-4.69094372 +1	-2.17711222 +1
H	5.50942491 +1	-5.87328116 +1	-2.71470875 +1
H	5.78165849 +1	-4.07377885 +1	-2.90933757 +1
H	4.33097217 +1	-5.95644000 +1	-0.03833017 +1
H	5.90078259 +1	-5.94975689 +1	0.91511987 +1
H	5.76414804 +1	-6.93477207 +1	-0.62663652 +1
H	-6.81454464 +1	-1.00939116 +1	-1.36563517 +1
H	-8.35099722 +1	-0.71149670 +1	-0.48364062 +1
C	-7.81243289 +1	-2.82136304 +1	-0.83435488 +1

H	-7.73534480 +1	-2.94728069 +1	-1.95608421 +1
N	-9.19133599 +1	-3.29764054 +1	-0.45036586 +1
H	-7.07440964 +1	-3.52621515 +1	-0.35131022 +1
C	-9.51556070 +1	-4.49301735 +1	-1.29606650 +1
C	-10.23259069 +1	-2.25931867 +1	-0.69432375 +1
C	-9.22557452 +1	-3.71112301 +1	0.98176507 +1
H	-10.19158439 +1	-1.47412841 +1	0.10614007 +1
H	-11.24749077 +1	-2.74144948 +1	-0.66424753 +1
H	-10.06777508 +1	-1.79373804 +1	-1.70173433 +1
H	-9.60319456 +1	-4.17301217 +1	-2.36772620 +1
H	-10.49149299 +1	-4.92684837 +1	-0.95224355 +1
H	-8.70073363 +1	-5.25473568 +1	-1.18691974 +1
H	-8.91115128 +1	-2.85419134 +1	1.63014220 +1
H	-10.27250765 +1	-4.01573974 +1	1.25124717 +1
H	-8.53148278 +1	-4.57934876 +1	1.13581123 +1

References

[1] S. Takahashi, Y. Kagami, K. Hanaoka, T. Terai, T. Komatsu, T. Ueno, M. Uchiyama, I. Koyama-Honda, N. Mizushima, T. Taguchi, H. Arai, T. Nagano, Y. Urano, *J. Am. Chem. Soc.* **2018**, *140*, 5925–5933.

[2] L. Štacková, P. Štacko, P. Klán, *J. Am. Chem. Soc.* **2019**, *141*, 7155–7162.

[3] H. Hyun, E. A. Owens, H. Wada, A. Levitz, G. Park, M. H. Park, J. V Frangioni, M. Henary, H. S. Choi, *Angew. Chem. Int. Ed.* **2015**, *54*, 8648–8652; *Angew. Chem.* **2015**, *127*, 8772–8776.

[4] Z. Wu, P. Shao, S. Zhang, M. Bai, *J. Biomed. Opt.* **2014**, *19*, 036006.

[5] D. Su, C. L. Teoh, A. Samanta, N.-Y. Kang, S.-J. Park, Y.-T. Chang, *Chem. Commun.* **2015**, *51*, 3989–3992.

[6] J. Cha, R. R. Nani, M. P. Luciano, G. Kline, A. Broch, K. Kim, J.-M. Namgoong, R. A. Kulkarni, J. L. Meier, P. Kim, M. J. Schernmann, *Bioorg. Med. Chem. Lett.* **2018**, *28*, 2741–2745.

[7] S. Ohnishi, S. J. Lomnes, R. G. Laurence, A. Gogbashian, G. Mariani, J. V. Frangioni, *Mol. Imaging* **2005**, *4*, 172–181.

[8] H. Hyun, M. W. Bordo, K. Nasr, D. Feith, J. H. Lee, S. H. Kim, Y. Ashitate, L. A. Moffitt, M. Rosenberg, M. Henary, S. K. Chio, J. V. Frangioni, *Contrast Media Mol. Imaging* **2012**, *7*, 516–524.

[9] M. Y. Berezin, K. Guo, W. Akers, J. Livingston, M. Solomon, H. Lee, K. Liang, A. Agee, S. Achilefu, *Biochemistry* **2011**, *50*, 2691–2700.

[10] H. J. Gruber, C. D. Hahn, G. Kada, C. K. Riener, G. S. Harms, W. Ahrer, T. G. Dax, H.-G. G. Knaus, *Bioconjug. Chem.* **2000**, *11*, 696–704.

[11] M. Grabolle, R. Brehm, J. Pauli, F. M. Dees, I. Hilger, U. Resch-Genger, *Bioconjug. Chem.* **2012**, *23*, 287–292.

[12] J. J. P. Stewart, *MOPAC*; Stewart Computational Chemistry: Colorado Springs, CO, 2008.

Author Contributions

DHL designed and synthesized **s775z**, carried out syntheses and characterization of literature dyes and RDG conjugates, measured photophysical properties and Xenon lamp photostability, performed molecular modeling. CLS synthesized and characterized **s775z-IgG** and **756z-IgG**, measured imaging station photostability and chemical stability, performed all the cell and animal imaging studies. BDS conceived the project, supervised the research, and wrote the manuscript.